AD-A056 387 SRI INTERNATIONAL MENLO PARK CA F/G 17/8
OPTICAL DIAGNOSTICS FOR THE STRESS EXPERIMENT PROJECT STRESS.(U)
NOV 77 R D HAKE, N J CHANG DNA001-76-C-0300
UNCLASSIFIED DNA-4487F NL

| OF |
AD
A056387

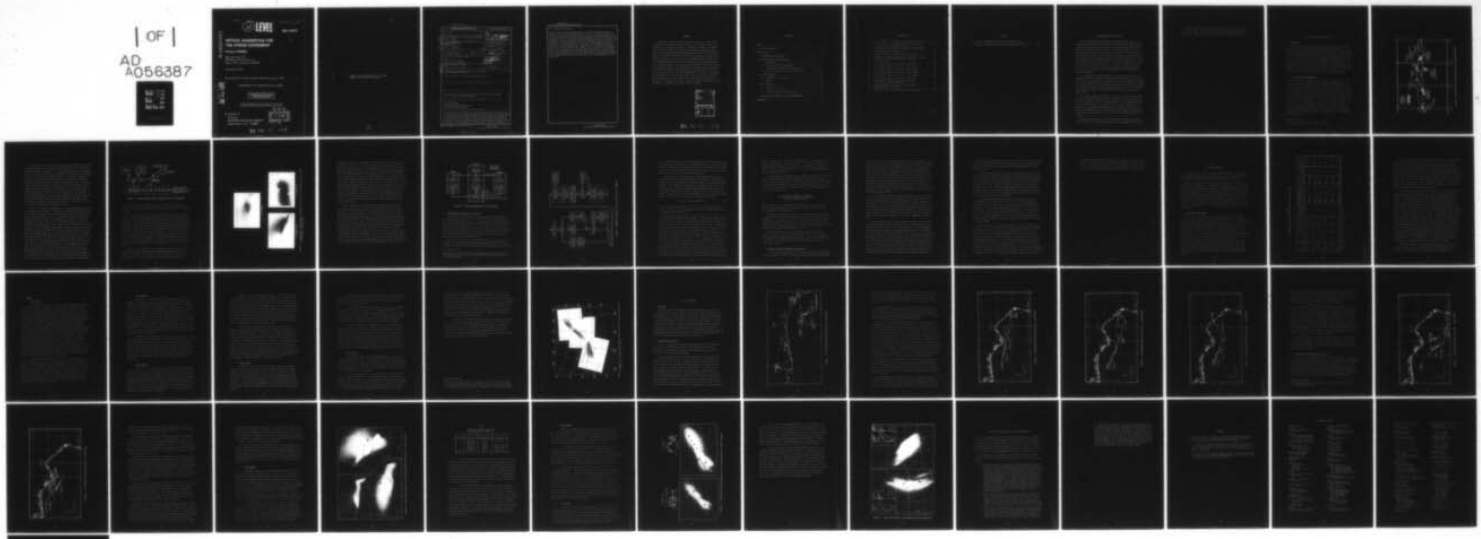

END
DATE
FILMED
9-78
DDC

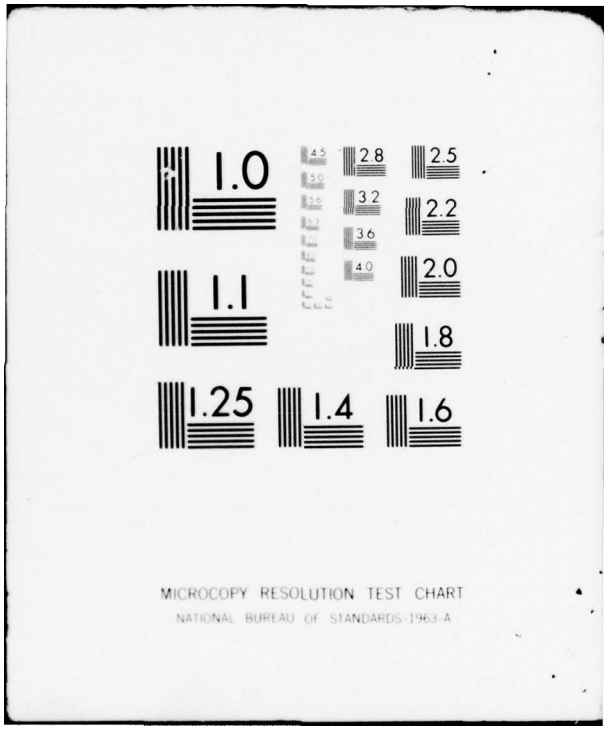
1.0
1.1
1.25
1.4
1.6
1.8
2.0
2.2
2.5
2.8
3.2
3.6
4.0
4.5
5.0
5.6
MICROCOPY RESOLUTION TEST CHART
NATIONAL BUREAU OF STANDARDS-1963-A

DNA 4487F

OPTICAL DIAGNOSTICS FOR THE STRESS EXPERIMENT

Project STRESS

SRI International
333 Ravenswood Avenue
Menlo Park, California 94025

November 1977

Final Report for Period May 1976—November 1977

CONTRACT No. DNA 001-76-C-0300

THIS WORK SPONSORED BY THE DEFENSE NUCLEAR AGENCY
UNDER RDT&E RMSS CODE B322076462 L25AAXHX63509 H2590D.

Prepared for
Director
DEFENSE NUCLEAR AGENCY
Washington, D. C. 20305

Destroy this report when it is no longer needed. Do not return to sender.

AD56 387

UNCLASSIFIED

SECURITY CLASSIFICATION OF THIS PAGE (When Data Entered)

REPORT DOCUMENTATION PAGE

READ INSTRUCTIONS BEFORE COMPLETING FORM

1. REPORT NUMBER: DNA 4487F
2. GOVT ACCESSION NO.:
3. RECIPIENT'S CATALOG NUMBER:

4. TITLE (and Subtitle): OPTICAL DIAGNOSTICS FOR THE STRESS EXPERIMENT Project STRESS
5. TYPE OF REPORT & PERIOD COVERED: Final Report, May 1976—Nov 1977
6. PERFORMING ORG. REPORT NUMBER: SRI Project 5378

7. AUTHOR(s): Richard D. Hake, Jr. Norman J. F. Chang
8. CONTRACT OR GRANT NUMBER(s): DNA 001-76-C-0300

9. PERFORMING ORGANIZATION NAME AND ADDRESS: SRI International 333 Ravenswood Avenue Menlo Park, California 94025
10. PROGRAM ELEMENT, PROJECT, TASK AREA & WORK UNIT NUMBERS: Subtask L25AAXHX635-09

11. CONTROLLING OFFICE NAME AND ADDRESS: Director Defense Nuclear Agency Washington, D.C. 20305
12. REPORT DATE: November 1977
13. NUMBER OF PAGES: 54

14. MONITORING AGENCY NAME & ADDRESS(if different from Controlling Office): DNA, SBIE
15. SECURITY CLASS. (of this report): UNCLASSIFIED
15a. DECLASSIFICATION/DOWNGRADING SCHEDULE:

16. DISTRIBUTION STATEMENT (of this Report)

Approved for public release; distribution unlimited.

17. DISTRIBUTION STATEMENT (of the abstract entered in Block 20, if different from Report)

18. SUPPLEMENTARY NOTES

This work sponsored by the Defense Nuclear Agency under RDT&E RMSS Code B322076462 L25AAXHX63509 H2590D.

19. KEY WORDS (Continue on reverse side if necessary and identify by block number)

Barium Releases
Ion-cloud Tracking
Incoherent-Scatter Measurements
Television Tracking Systems

20. ABSTRACT (Continue on reverse side if necessary and identify by block number)

A three-site television-aided tracking network was constructed and fielded for the STRESS series of barium releases. The real-time tracks of the barium-ion clouds were used to deduce the ground locations where the coverage of a communications satellite would be affected by the structured ionization in the clouds, so that an instrumented test aircraft could be vectored to these locations. Six releases were successfully tracked during the December 1976 through March 1977 test windows. The TV network acquired the barium-ion

DD FORM 1 JAN 73 1473 EDITION OF 1 NOV 65 IS OBSOLETE

UNCLASSIFIED

SECURITY CLASSIFICATION OF THIS PAGE (When Data Entered)

410281

20. ABSTRACT (Continued)

clouds as early as times corresponding to a 3° solar depression angle and maintained track until the sun set on the cloud 40 to 45 minutes later. The differences between cloud tracks generated by this television network and by an incoherent scatter radar that had also tracked the clouds could usually be ascribed to the two systems intentionally focusing on different regions of the amorphous ion cloud, and did not arise from inconsistencies in the tracking algorithms. Operating experience of the TV-tracking system showed that the most useful tracking procedure for experiments such as STRESS, though not necessarily the most accurate, was a single-site track that uses an empirical model for the cloud altitude after release. Projection of the second DIANNE rocket probe trajectory onto cloud photographs from various ground stations showed that the rocket did not encounter the region of peak electron density in its passage through the cloud. The radar-derived electron density profiles could be related to specific ion-cloud features for event ESTHER, but not for event FERN.

PREFACE

Archibald V. McKinley was the innovative architect of the system hardware, ably carrying it from the design stage through construction, installation, and field maintenance. Marilyn F. Williams very capably contributed the software, and persisted diligently throughout several courses of externally-imposed, last-minute alterations in that software. McKinley, Williams, and Billy P. Ficklin, who operated the Tyndal site, contributed beyond the call of dury in contending with the Florida telephone companies and a particularly cold November to complete and debug the field installation. We are especially grateful to Victor H. Gonzalez for contributing many of the triangulation algorithms and for providing the incoherent-scatter radar data during the analysis phase, as well as helping in the analysis. We also thank Wallace P. Boquist of Technology International Corp. for the use of two lenses during the tests and for the photographs of the ion clouds used in the Section III analysis. Finally, we acknowledge the support and encouragement of Major B. W. Motal and Major R. A. Bigoni, the project officers at DNA.

CONTENTS

ILLUSTRATIONS

TABLES

I INTRODUCTION AND OVERVIEW

Project STRESS (Satellite TRansmission Effects SimulationS) was a communication experiment sponsored by the Defense Nuclear Agency (DNA) in cooperation with the Air Force Electronics System Division (ESD) and the Air Force Avionics Laboratory (AFAL). The principal purpose of the experiment was to evaluate the performance of satellite communication links under perturbed conditions that simulate many aspects of a post-nuclear-burst environment. This perturbed environment was produced by the use of artificial barium ion clouds released at an altitude of 185 km. An NC-135 test aircraft, receiving signals from a synchronous communication satellite, was directed to fly a course during which the signal path passed through the ionized barium cloud while measurements were made of data transmission quality.

The experiment scenario depended on ground-based radar and optical instrumentation for tracking the barium cloud. The position of the shadow cast by the barium cloud on the ground coverage of the communications satellite was determined, and then displayed on the CRT screen of an air-traffic controller, along with the radar-determined position of the test aircraft. The air-traffic controller then vectored the aircraft to intercept the shadow region.

The overall program consisted of one release in early December 1976, and five releases during late February and March 1977, all at Eglin Air Force Base, Florida. The release in December, code named ANNE, was used to test the performance of the individual test element hardware and the ability of those elements working in concert to maneuver the aircraft into the cloud-shadow region. Modification of the hardware or the interface procedures was performed in the interim period before the five 1977 releases.

This report deals with the television-aided tracking system (hereafter referred to as the TV-track system) used to determine the cloud and

cloud-shadow positions during the twilight period when the clouds were optically visible. Design objectives, hardware construction, field operation, and data reduction are discussed in the following sections.

II SYSTEM DESIGN AND CONSTRUCTION

A. Background

The overall design of the TV-track system was based on a similar system[1]* used by the University of Alaska during the SECEDE-II series of barium releases conducted at Eglin AFB during early 1971. In the SECEDE-II series, the TV system's primary purpose was to generate a cloud-track that was used in real-time to vector a photographically-instrumented aircraft to the foot of the magnetic field line passing through the cloud. The successful operation of that TV system established a high degree of confidence in optical tracking systems in general. The problems encountered during that system's real-time operation were extremely useful in establishing the successful netting philosophy for the STRESS releases.

B. Siting, Netting, and Hardware

It was decided to again establish TV-track observing sites at three locations, to provide redundance in the cloud-triangulation procedure, as well as to provide a backup capability in the event of cloud cover obscuring one site. No reason was found to change the locations from those used during SECEDE-II. Those sites are separated by baselines of nearly 100 km, appropriate to high-resolution triangulation from a 200-km range to the releases. The TV-track sites, located at Tyndall Air Force Base site 9702, Eglin AFB site C-6, and the Barin Field Naval Air Station, are shown in Figure 1 along with other elements of the STRESS experiment matrix.[2] Also shown in Figure 1, are a generalized box model of a barium cloud (assumed to be centered at 185 km altitude) and the positions of the ground shadow of that cloud appropriate to the pre-STRESS and STRESS tests.

---

*References are listed in the Reference section.

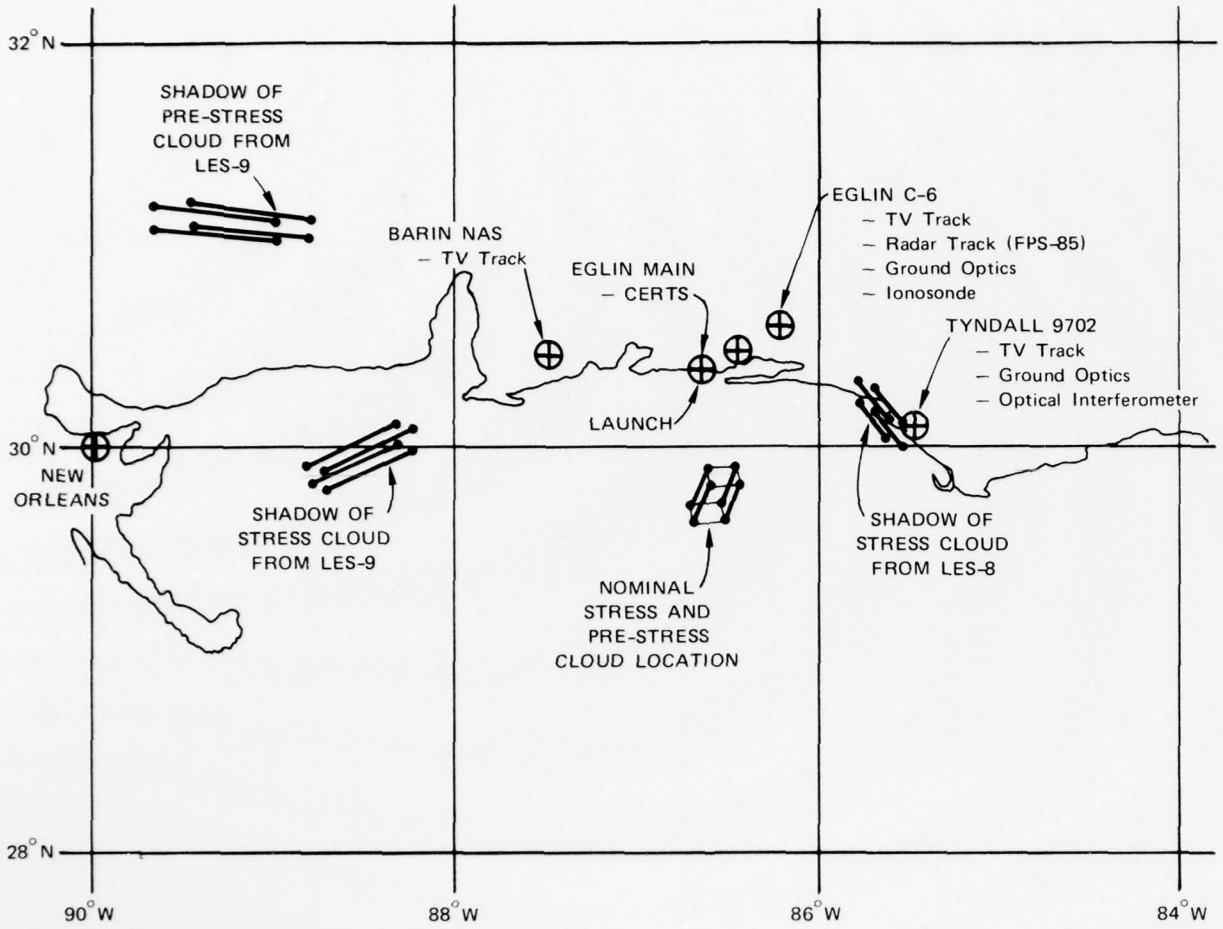

FIGURE 1 PROJECT STRESS: INSTRUMENT, CLOUD, AND SHADOW LOCATIONS

Note that the C-6 TV site was collocated with the FPS-85 Space Track Radar, which was used to perform the radar track[3] of the ion clouds by incoherent-scatter techniques. Site C-6 was established as the principal site of the TV net, containing the triangulation computer and the contact point for the balance of the STRESS matrix. Under normal operating conditions, the TV-derived ion-cloud position was relayed to the FPS-85 radar installation by means of acoustic-ccupled phone lines. The FPS-85 computer then projected the cloud position from the satellite line-of-sight with the same algorithms used to generate a cloud shadow from the radar-derived cloud position. The TV-derived cloud and cloud-shadow positions were then relayed to the various STRESS users by personnel inside the FPS-85 building. The primary cloud-data user was the aircraft-controller, located at CERTS on the Eglin main base. Secondary users were personnel associated with the probe-rockets at the launch site, and the optical interferometer at Tyndall site 9702.

Figure 2 is a schematic diagram of the tracking hardware at each site. A low-light-level TV camera [Cohu Model 4410, Silicon-Intensified-Target (SIT) camera] was mounted on a motor-driven platform with remote controls for setting azimuth and elevation. Azimuth and elevation readouts were digitized to 14-bit accuracy for display and for input to the central triangulation computer at site C-6. The digital look-angle data were transmitted from the "wing" sites (Tyndall and Barin) to the TV-net central computer at C-6 on commercial phone lines by means of acoustic couplers. The central computer (HP-2100) performed the triangulation of the cloud position using data from one, two, or all three of the sites according to selection procedures and algorithms discussed in Section II-C, below. It then computed the look angles of this theoretical cloud location as seen from each site and transmitted these angles back to each site along the same phone lines used for the data input. The look-angle data, along with an electronically-generated boresight reticle, were stored in a matrix memory device at each site. The contents of the matrix memory were continuously mixed with the video from the camera and displayed on the monitor screen. The operator was thus provided with video imagery of the cloud, overlaid with a boresite and the computed cloud position

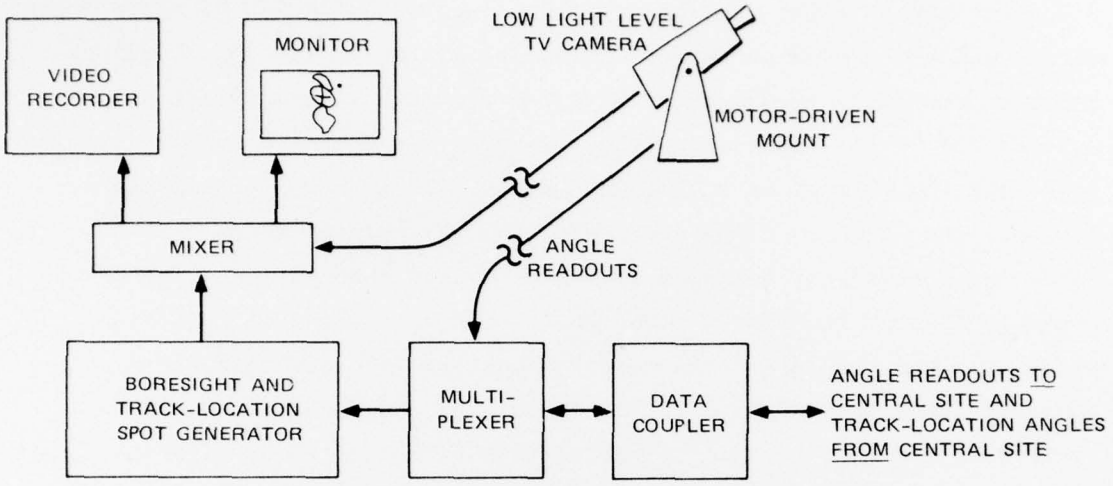

FIGURE 2 BLOCK DIAGRAM OF SITE EQUIPMENT FOR TV-TRACK SYSTEM

as seen from his site. In addition to its own boresight, the C-6 TV monitor displayed the central portions of the Barin and Tyndall boresight overlays.

The TV tube in the Cohu cameras was an RCA SIT vidion with a 16-mm format. The cameras were equipped with f/0.95, 50-mm focal-length lenses (Schneider "Xenon" Model CM120), giving a TV field of view roughly 10.5° (vertical) by 14° (horizontal). A narrowband interference filter (26.5 Å full-width at half maximum, 4563 Å peak wavelength, 58% peak transmission) was used to isolate the 4554 Å line and enhance the visibility of the ion cloud when viewed against the bright twilight sky. These filters could be manually placed over the TV-camera lenses, and permitted acquisition of the cloud 5 to 10 minutes earlier than would otherwise have been possible. By blocking out the light from the neutral cloud, the ion filters also helped in identifying the early development of structure in the ion cloud.

Figure 3 is an example of the video imagery available at each site; these pictures were taken from event DIANNE at 0034 GMT (release + 32 minutes, 50 seconds). The sequence of bars and dots across the top of each screen is a time code, which was also stored and updated in the

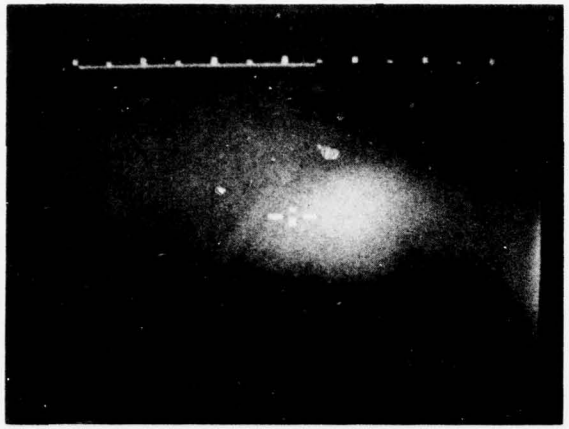

(a) C-6 VIEW

(b) TYNDALL VIEW

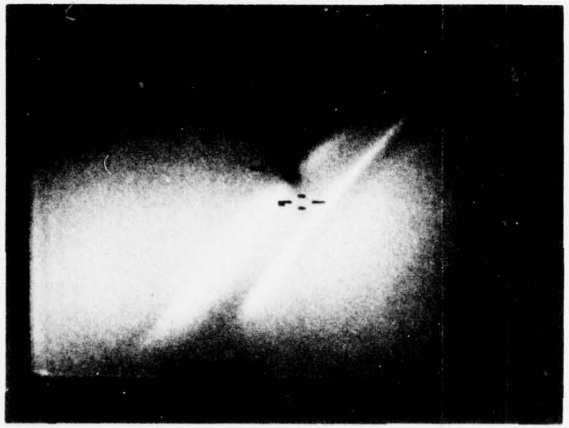

(c) BARIN VIEW

FIGURE 3 TV IMAGERY OF EVENT DIANNE AT 0034 UT (R + 32 min, 50 s) AS RECORDED ON VIDEO TAPE AT THE THREE TV-TRACK SITES

matrix-memory device. The length of the lower bar in the time code increased one step at the change of the minute and an upper bar (absent in this case) showed the hour. In the Tyndall screen, the computed cloud position is the short bar just to the lower left of the ion-cloud luminosity. The boresight reticle is the group of two short and two long bars near the center of the screen. In the Barin screen, the boresight reticle and computed cloud position (short bar touching the left-hand bar of the reticle) are visible, along with a burn spot on the TV-camera tube (central dark blotch), and spurious bits injected into the matrix memory by interference on the C-6/Barin data-line phone connection (long bar just to the left of the burn spot). In the C-6 screen, the boresight reticles and computed cloud positions from Tyndall and Barin are overlaid onto the lower left and right (respectively) corners to show the scientific director at C-6 the magnitude and sense of the tracking discrepancies at the two wing sites.

Figure 4 shows how the hardware and operators of the three sites were netted to provide the needed real-time feedback in the tracking procedure. Each site operator was responsible for maintaining a steady track on the relevant portion of the ion cloud as it evolved in time. The scientific director viewed the C-6 display, and received information orally from the wing-site operators concerning the gross structure of the cloud as seen from their site. The scientific director then determined, on the basis of this information from the wing sites, visual imagery of the cloud as seen from C-6, and the visual overlay of the boresight/computer-track-point discrepancies at all sites, whether each site should maintain track on their chosen part of the cloud, or should shift emphasis to a different portion of the cloud. This real time feedback was quite necessary because of the differing appearance of the diffuse, geometrically complex barium clouds from the three widely-separated points of view.

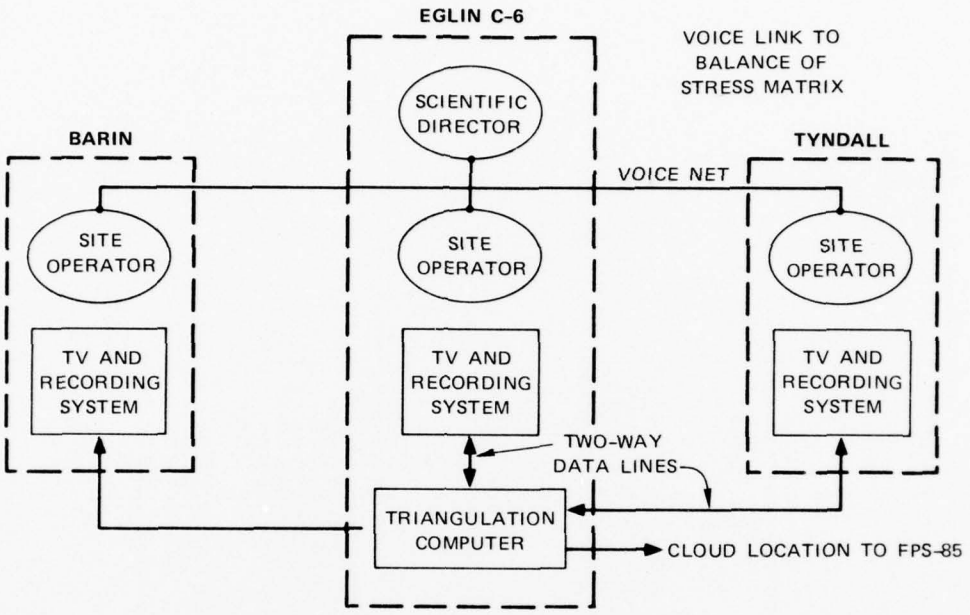

FIGURE 4 NETTING DIAGRAM FOR TV-TRACK SYSTEM

C. Triangulation Algorithm and Software

Figure 5 is a flow chart of the internal tracking loop used by the TV-track computer at the C-6 site.* The left side of the figure shows the three alternate paths available for computing the cloud position, depending upon whether one, two, or three of the TV sites were active at the time. The selection of active sites was made in real time by front-panel switches operated by the C-6 operator on the basis of sky and hardware conditions at each site. The right side of the figure shows the uses made of the computed cloud position.

Under normal conditions, the TV-track shadow given to the aircraft controller was calculated by the FPS-85 computer because of the higher-accuracy algorithms and satellite-position data available in that facility.

*The software of Figure 5 was fully operational only for the latter five STRESS releases. See Section III-A for differences during the first release (event ANNE).

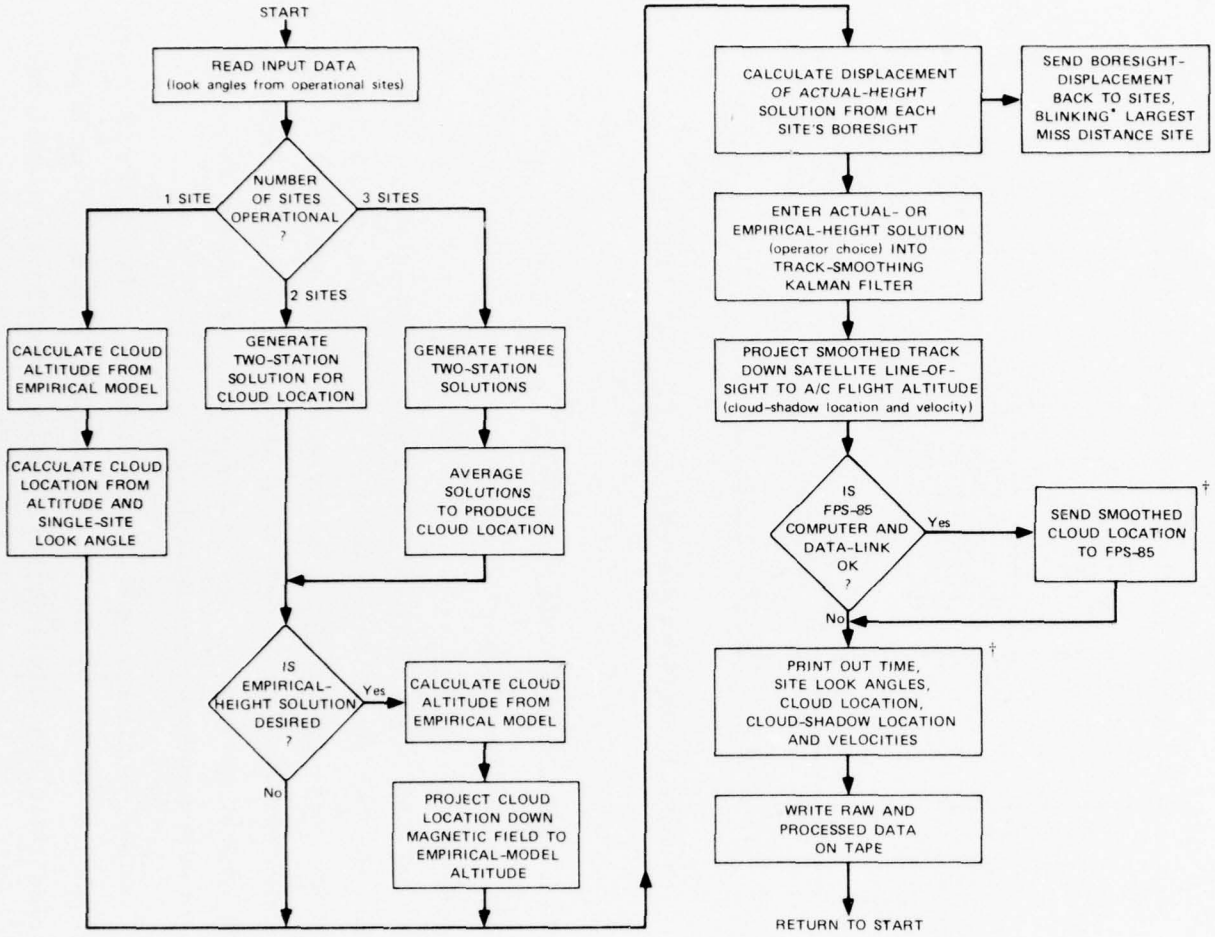

*Omit blinking if only 1 or 2 sites active.

†These steps are under buffer control, i.e., the computer enters data into a buffer and then procedes to the next step before the printout or data transmission is completed.

FIGURE 5 PROGRAM FLOW CHART FOR TV-TRACK CENTRAL COMPUTER

The TV track computer generated and printed its own cloud-shadow position at all times, as a backup in case the FPS-85 computer or data link failed. TV-track cloud position was smoothed before being presented to the FPS-85, because the TV-track interface was limited to a data rate that would have greatly under-sampled the available TV-track data.

The algorithm for determining the cloud-location from single-site observations was to take the point where the look-angle vector from the single active site penetrated a spherical surface at the empirical-model altitude. (The empirical-cloud altitude actually was taken to be the distance above a geocentric sphere passing through the C-6 site.) For events ANNE and BETTY, the empirical model held the cloud altitude constant at a height of 185 km. For subsequent events, the empirical height formula used for the cloud altitude as a function of time was:

$$h = 140 + 45 \exp(-0.0001633\ t) \qquad (1)$$

where h is the cloud altitude in km, and t is the time after release in seconds. Equation (1) is an empirical fit to the cloud-altitude data of event ANNE from the radar track.

The algorithm for generating a cloud location with two active sites, called A and B for example, was as follows. First, define a plane by the vectors AB and AC, with the vector AB running between the two active sites and AC being the pointing vector from site A to the cloud. Second, assume (to first order accuracy) that the pointing vector BC from site B to the cloud lies in that same plane, thus defining a triangle ABC where C is the intersection of the two pointing vectors. In this procedure, the angle CBA is maintained the same as the angle between the intersite vector BA and the true pointing vector from site B. (Another way of looking at it is that the pointing vector from site B to the cloud is rotated in space, about an axis BA running between the two sites, until it lies in the plane defined above.) Third, solve that triangle for the distance AC and BC; i.e., the distances from each site to the first-order location of the cloud. Fourth, determine the locations in space of the points lying along the true pointing vectors and at distances AC and BC from sites

A and B, respectively. Call these points C′ and C″, respectively. (Note that with the geometry as defined above, C′ and C will be identical.) Fifth, take the two-station solution to be the midpoint of the line between C′ and C″, and the distance C′C″ is defined as the miss-distance of that two-station solution.

The algorithm for generating a cloud location with three active sites starts by calculating the three independent two-station solutions and their associated miss distances. These three positions are then averaged in a manner that weights each two-station solution according to the inverse of its miss distance. The formula for this average, assuming sites A, B, and C are active, is:

$$\bar{P} = \frac{\sigma_{BC}\sigma_{AC}\bar{P}_{AB} + \sigma_{AB}\sigma_{AC}\bar{P}_{BC} + \sigma_{AB}\sigma_{BC}\bar{P}_{AC}}{\sigma_{AB}\sigma_{AC} + \sigma_{AB}\sigma_{AC} + \sigma_{BC}\sigma_{AC}} \qquad (2)$$

where $\bar{P}$ is the vector three-station solution, $\bar{P}_{AB}$ is the vector two-station solution using pointing angles from sites A and B, and σ_{AB} is the associated miss distance, etc.

The computer operator has the option of normalizing either the two-station solution or the three-station solution to the empirical height appropriate to that time. To do this, the calculated position is translated along a magnetic field line (i.e., along the axis of the cloud striations) to the appropriate height. The field line was taken as having a 61° dip angle and a 3° declination to the east.

The time constant of the track-smoothing filter referred to in Figure 5 was chosen to be about three minutes. This value eliminated most of the unintentional operator tracking jitter, and yet allowed the track point to be shifted on a reasonable time scale from one area of the cloud to another.

D. System Evolution and Operating Experience

Several operational difficulties in this procedure became apparent as the test series evolved. Integrating the oral and visual inputs from

the three sites into a useful picture of the ion cloud demanded the constant attention of the scientific director, to the exclusion of communicating with the balance of the STRESS experiment net. The manual task of actually tracking the cloud at C-6, on the other hand, was quite simple, and coincidentally demanded the same kind of attention to the cloud evolution as was already required of the scientific director. The scientific director therefore took on the role of C-6 operator as well. The second person at C-6 was then able to devote full attention to the triangulation computer, monitoring the behavior of the computed track point, and relaying cloud-track data intermittently to other STRESS experimenters. This division of duties was much more satisfactory than the division portrayed in Figure 4.

A less remediable operating difficulty became more and more evident as the test series continued. This involved the extreme difficulty of orally conveying sufficient information about the cloud's appearance on the wing-site monitors to allow the scientific director to swiftly develop a feeling for the very complex three-dimensional cloud, and to determine where on that cloud each site was pointing. It was usually only after seeing each site's video tapes of the event that the scientific director was able to fully appreciate the cloud's appearance from each site.

The oral communication of visual imagery between the sites did improve throughout the course of the test series, but the learning curve was too slow to be effective for a six-test series. It is now apparent that this problem could have been properly addressed only by relaying the video imagery of the wing sites back to the central site so that the scientific director could see all three views of the cloud simultaneously. This would allow the director to acquire a much better feeling for the cloud's shape, and for which part of the image should be tracked by each site. More importantly, it would allow the director to advise each site operator in a visual reference frame common to both. For instance, an instruction to a site operator to "move your aim point 45° upward and to the right by half an inch" is much more useful than an instruction to

"move about halfway back toward the tail of the cloud." This is especially true when the site operator is not sure whether the tail of the cloud is upscreen or downscreen on the display at that particular time, as was often the case.

A third operational difficulty that became apparent during the test series was that the Barin site was generally of very little use. Because of its brighter sky, Barin acquired the cloud much later than Tyndall and C-6, and always had a much less distinct view of the cloud. By the time the Barin sky was dark enough for optimum viewing, the sun was already setting on the cloud. The Barin general picture of the cloud was occasionally helpful in steering the Tyndall and C-6 combination up and down the field lines, but this did not happen often enough for the site operation to be merited on those grounds alone.

In initial STRESS planning it was thought advisable to place the third TV-track site somewhere to the west of C-6 to be prepared for a westward drift of the ion cloud. It was thought that the STRESS clouds released 2 to 4 hours before sunset might be blown to the west and require a site such as Barin for optimum observation. It is now apparent that an eastward ion-cloud drift near sunset at Eglin is a virtual certainty. A third triangulation site to the east of Tyndall would have been preferable, and should be adopted in the event of future test series similar to STRESS.

Another comment about siting preferences is that the Tyndall to C-6 baseline was not long enough for an effective real-time height determination of the cloud. When the cloud was midway between the two sites, neither site had a sufficiently orthogonal view of the cloud's extent along the field lines to suitably restrict the altitude variability of the computed cloud location. Another way of stating the problem is that the opening angle between the C-6 and Tyndall pointing vectors to the cloud was so small that the random differences in target objects chosen by the two sites gave large altitude variations in the computed two-station solution. Although the Tyndall to C-6 baseline is suitable for post-event triangulation of fine-scale features, it was not optimum for real-time

triangulation of medium-sized regions of the cloud. For future tests, it would be desirable to use a site emplaced considerably farther east of Tyndall. In addition to providing a larger baseline, the earlier sunset of such a site would permit earlier optical acquisition of the cloud.

III SYSTEM OPERATION

This section of the report contains a brief description of the operation of the TV net during each of the six releases. The cloud-position tracks obtained during the operations are discussed in Section IV.

Table 1 is a summary of the temporal data for the six releases. Notice that the progression of release time was from late to early. ANNE was released at 96° SDA when the experience of SECEDE showed that the sky was dark enough to permit a continuous optical track following the release. Succeeding releases were made progressively earlier, so that the clouds could be documented during the twilight optical window at progressively later stages in their evolution. As the series progressed, the TV net acquired the cloud at earlier times, and consistently acquired the later clouds at about an SDA of 3°. The track duration in most cases was about 40 minutes.

A. Pre-STRESS: Event ANNE

Water clouds were present at all three sites during event ANNE, which interfered with the TV imagery to varying degrees. At Barin, the barium cloud was obscured almost completely by overcast, being discernible only during the flash as the barium was released, and for a few intermittent periods of seconds at later times. The deleterious effect of the overcast at Barin was compounded by the fact that the barium cloud was within a few degrees of the nearly-full moon. The overcast was considerably thinner at C-6 and Tyndall, where the release was clearly observed and the barium cloud position was obscured only intermittently. The cloud track was generated by two-station tracking from C-6 and Tyndall. Track was initiated immediately after release and continued for about 30 minutes before the cloud began to fade. The cloud was finally lost from the C-6 site 35 minutes after release, and from Tyndall somewhat earlier.

Table 1

SUMMARY OF STRESS TEMPORAL DATA FOR TV-TRACK SYSTEM

Event	Date	Time of SDA* = 6°, GMT	Release Time, GMT	Interval by Which Release Preceded SDA 6° (minutes)	TV-Net Acquire		TV Loss of Track, GMT (Time After Release)	Track Duration (minutes)	Last View of Cloud, GMT
					Time, GMT (Time After Release)	SDA (deg)			
ANNE	12/1-2/76	2312	2311:42	0	2311 (R+0 min)	6	2341 (R+30 min)	30	2344
BETTY	2/26-27/77	0006	2352:27	13	0003 (R+11 min)	5.3	0040 R+48 min)	37	0040
CAROLYN	3/2-3/77	0009	2354:10	15	0000 (R+6 min)	4	0040 (R+46 min)	40	0042
DIANNE	3/7-8/77	0012	0001:08	11	0001 (R+0 min)	3.5	0042 (R+41 min)	41	0045
ESTHER	3/13-14/77	0016	2301:09	75	0002 (R+61 min)	2.8	0044 (R+103 min)	42	0047
FERN	3/14-15/77	0017	2246:09	91	0004 (R+78 min)	3.2	0046 R+120 min)	42	0052

*SDA = solar depression angle, referenced to Site C-6.

Post-event analysis of the TV-track data showed that the two-station solution agreed quite well with the FPS-85 radar track. The TV-track data sent to the FPS-85 was misinterpreted within the FPS-85 computer; the latitudinal and longitudinal displacements from the reference location were interchanged. This resulted in the optically-derived cloud-shadow locations being considerably in error. The aircraft followed the optically-derived shadow and gathered no data for the first 27 minutes of cloud life. Fortuitously, the true cloud-shadow and the shadow derived from the interchanged data crossed paths at that time and the aircraft began acquiring data. Shortly afterwards, the sun set on the cloud and the aircraft was directed to follow the radar-derived cloud track.

A further difficulty during event ANNE was the occurrence of large and apparently random excursions of the shadow on the ground, making it difficult for the aircraft to intercept the optically-derived cloud shadow. This problem was traced to the random altitude excursions of the two-station C-6 and Tyndall solution as the two sites tracked the cloud. These altitude excursions were magnified in projecting the cloud location down to the shadow location, and the subsequent erratic behavior of the shadow prevented the air traffic controller from accurately directing the aircraft to intercept cloud shadow. The solution to this problem was to allow the triangulated cloud position to assume any altitude, but to translate that position along the earth's magnetic field lines to a smoothly-varying cloud-center altitude before generating a cloud shadow (empirical-height solution in Figure 5). Furthermore, since the data-rate of the link from the TV-track computer to the FPS-85 was not able to pass each independent TV determination of the cloud location, it was decided to pass the TV-track data through a smoothing filter before presentation to the FPS-85 computer. The TV track software flow chart given in Figure 5 is thus appropriate to the system as it operated in the latter five STRESS releases, rather than for event ANNE.

In summary, the TV-track system performed during event ANNE in a manner that revealed several problems with the system and its use, but showed no major obstacles to its successful use in STRESS per se.

B. STRESS

1. Event BETTY

Event BETTY also occurred under less-than-optimum sky conditions, with light overcast at Tyndall and C-6, and light to heavy overcast at Barin. The actual release was not observed on any of the TV systems, as it occurred considerably to the south of the anticipated location. Event BETTY was the first barium-ion cloud to be released at a solar depression angle (SDA) of less than 6°, and hence was subject to somewhat of a learning experience in adapting to the brighter sky-background conditions. C-6 was the first TV site to acquire the cloud, at R + 11 minutes. A single-site track was initiated at that time with the cloud altitude being fixed at 185 km (the empirical-model software for cloud-altitude falling as a function of time was not operational for event BETTY). Most of the early cloud track was generated by the C-6 single-site track because Tyndall and Barin had only intermittent views of the cloud. Barin had rain shower about R + 26 minutes, for which the equipment had to be covered, and the Barin site was generally useless during the entire event. Tyndall visibility improved substantially near R + 35 minutes and a two-station track was used for the next 10 minutes. Site C-6 became completely overcast at R + 46 minutes, shortly before the sun set completely on the cloud as observed from Tyndall at R + 48 minutes.

Again, the TV-track data was not useful to the aircraft controller, because two of the 32 coaxial cables connecting the TV-interface unit to the FPS-85 computer were interchanged during the experiment setup. This problem was identified during post-event data analysis, and was corrected by arranging to leave the interface unit connected to the computer for the remainder of the STRESS test window. The problem had not been detected before the release because last-minute changes in the release scenario necessitated foregoing some of the normal consistency-checks between the FPS-85 and TV-track computers.

2. Event CAROLYN

Visibility at Tyndall and C-6 was quite good for most of event CAROLYN, but Barin's view of the barium-ion cloud was somewhat degraded by cirrus. The actual release was seen by all sites and the ion cloud itself was first acquired by the Tyndall site at R + 6 minutes, followed by C-6 at R + 8 minutes. A two-station track was maintained until R + 30 minutes when the ion cloud became sufficiently distinct through the cirrus at Barin that a three-site track could be initiated. Low-altitude cumulus obscured the C-6 view of the ion cloud at R + 42 minutes, shortly before the TV-track was terminated by the sun setting on the cloud. The cloud faded from view at Tyndall at approximately R + 49 minutes. The southern edge of the ion cloud passed through the Tyndall magnetic zenith at ~R + 42 minutes, providing a magnificent view of some very narrow (N-S) and extremely long (E-W) sheets.

CAROLYN was a well-behaved ion cloud in the sense that a fairly well-defined group of striations formed at the head (trailing edge) of the cloud and maintained their identity as the cloud drifted to the east. Since this striation group was easily identifiable from all sites, and unquestionably the most interesting part of the cloud from a STRESS point of view, the TV track job was made considerably easier. The TV-track software and all interfaces worked well during event CAROLYN, resulting in an opical track that was quite smooth and usable by the aircraft controller.

3. Event DIANNE

Skies over all three TV sites were reasonably clear throughout the entire release. The release was again seen by all sites, and by this time, the site operators were sufficiently well experienced in finding the rather amorphous early cloud that the ion cloud was kept in continuous track following the release. The initial cloud track was a two-station (Tyndall and C-6) track. At R + 14 minutes, the skies became dark enough over Barin to make that site view useful and a three-station track was initiated. The optical track continued until R + 41 minutes; the cloud was lost from view around R + 44 minutes.

DIANNE was not a well-behaved ion cloud. It developed a kink near the midpoint, starting at about R + 16 minutes. The striations at the head (trailing edge) of the cloud moved out of the main body of the cloud much faster than the previous releases, resulting in a rather tenuous bunch of striations with an ill-defined center. An attempt was made to keep the TV-track aim point within the striated region at the head of the cloud, and closer to the unstriated main body from which the striations were emerging than to the lead striation. The tracking situation was further confused when a second striated region developed behind the kink, well away from the head of the cloud. This second group of striations was ignored in picking the TV-track target.

The TV-track cloud position was well behaved during event DIANNE, with the empirical height solution providing the smoothest track of any of the STRESS releases. Unfortunately, the FPS-85 computer went down at around R + 20 minutes, and the restart procedure introduced an erroneous coordinate-system zero into the software that handled the TV-track data. The TV-track data given to the aircraft controller were thus invalid after R + 20 minutes. This error was discovered around R + 30 minutes, and it would have been possible then to relay the TV-track cloud position directly to the aircraft controller without going through the FPS-85. The aircraft was successfully encountering the cloud shadow using radar cloud-tracking data alone, however, so the TV-track data were not used during the final 10 minutes of optical-track data.

4. Event ESTHER

ESTHER was the first of the two clouds released considerably before sunset. By the time the ion cloud became visible it was almost completely striated, and turned out to be a rather good object to track. There was a well-defined group of striations that maintained their identity, both collectively and individually, as the cloud drifted to the southwest. The occasional discontinuities in the optical track occurred because of a decision to change emphasis to a different part of the cloud, as the entire cloud became visible and its overall structure became more apparent.

Skies were quite clear throughout the event at Tyndall and C-6. There was a high, thin overcast at Barin, however, which resulted in the Barin picture being consistently fuzzy, with none of the well-defined structure seen at Tyndall and C-6.

The C-6 personnel noticed during the event that the striations at the head of the cloud seemed to become "less well defined" as the cloud aged, even while the relatively young striations near the center of the cloud remained visually sharp. If this qualitative impression could be strengthened by quantitative analysis of the ESTHER photographs, it would provide useful information on late-time striation morphology.

TV-track software, the FPS-85 interface, and the FPS-85 computer all worked well during event ESTHER. Differences in the optical and radar track were noted in real time and were ascribed to choosing different portions of the very large cloud to track. The radar-track remained smooth and continuous during the optical lifetime of the cloud, and, because the aircraft was successfully acquiring data, no need was seen to switch to the optical track during the visible cloud lifetime. Optical track of the cloud extended from R + 61 to R + 103 minutes, with the last vestige of cloud radiance lasting until about R + 106 minutes.

5. Event FERN

Event FERN was much like event ESTHER insofar as TV-track system operation was concerned. All sites were clear, the cloud was well striated as it became visible, and the Barin view of the cloud was marginally useful. Again, all TV hardware and software worked well and a solid track was maintained from R + 78 to R + 120 minutes. The cloud was no longer perceptible by R + 126 minutes.

An attempt was made to center the TV track on the easternmost area of structured luminosity. It was noticed that, as in the case of ESTHER, the TV track was east of the radar track, but it was assumed that the discrepancy was again caused by different, but equally valid, portions of the cloud being tracked. However, when the aircraft was directed to intercept the cloud-shadow generated from the optical track (at about

R + 70 minutes when the radar temporarily lost track on the cloud), the magnitude of the cloud-generated interference effects was observed to decrease markedly. We now believe this is because the TV net was tracking not the head of the main ion cloud, but the eastern end of the ion bridge,* which had had sufficient time since release to form striations of its own. This belief is based upon the low density of that region as observed by the aircraft, and upon the noticeably earlier fading of that region when compared to the main cloud region (implying a significant difference in altitude, and hence a different origin).

Figure 6 is a montage of three views of the cloud as seen from C-6 over a 90-second time span. Region A is the part of the ion cloud upon which the TV net focussed while tracking the cloud. Region B is assumed to be in the main ion cloud and is the portion of the cloud tracked by the FPS-85. Note that the azimuth and elevation lines in Figure 6 are only approximate, since the montage was created by overlaying TV pictures generated over a 90-second period.

---

*The term "ion bridge" denotes the nebulous region of barium ionization left by the neutral cloud as it is blown eastward of the main ion cloud. It is produced by photodissociation of BaO, followed by photoionization of the barium, and has a much lower ion density than the main ion cloud.

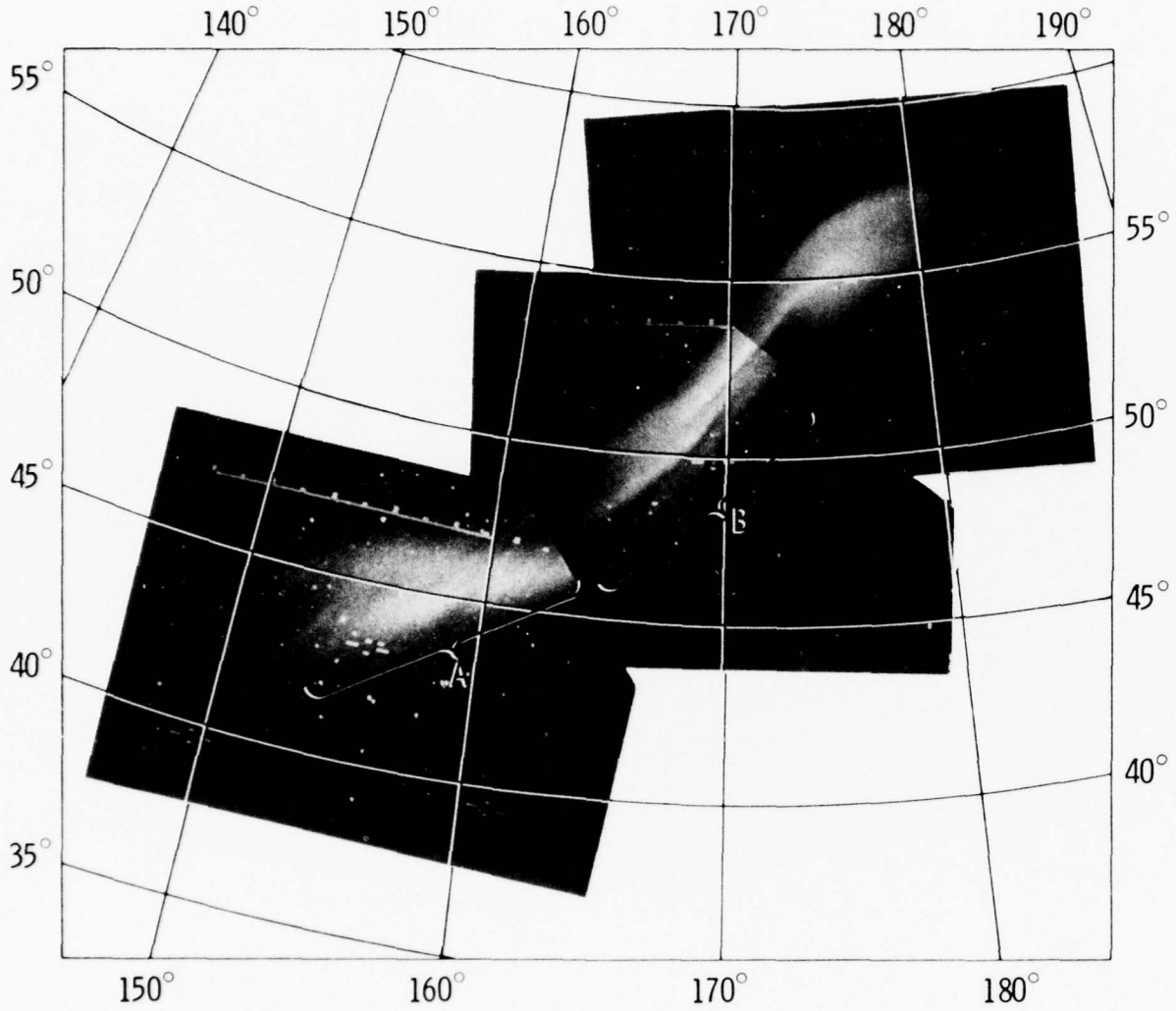

FIGURE 6 MONTAGE OF TV VIEWS OF FERN, AS SEEN FROM SITE C-6 DURING THE 0046 TO 0047:30 TIME PERIOD (R + 120 min to R + 121 min, 30 s)

IV DATA ANALYSIS

A. Overview

Analysis of the TV-track data was oriented toward two objectives. The first objective was to compare the optically- and radar-derived time-histories of the cloud locations to determine the nature and significance of any discrepancies. The second objective was to utilize the triangulation software developed in the course of the TV-track project to identify on cloud photographs the location of significant radar- and probe-derived cloud features. Work connected with the latter objective was closely coordinated with concurrent work at SRI on the STRESS radar track project.[3] Additional RF/optics data comparisons, especially of event DIANNE, will be found in forthcoming technical reports on that project.

B. Cloud-Track Location

Figures 7 through 12 show the ground projections of the cloud-track point for events ANNE through FERN. The TV-track data are given as heavy lines with ten-minute markers; the radar-track data are given as light lines with twenty-minute markers.

For event ANNE, Figure 7, the TV-track shows large North-South excursions about the radar track. These are caused by the cloud altitude computed from the two-station, Tyndall and C-6, solution moving up and down the field line upon which the cloud resided. As mentioned before, these altitude excursions produced large East-West excursions of the cloud-shadow location, a problem that inspired the implementation for events BETTY through FERN of the empirical-height solution. In addition to the North-South oscillations, Figure 7 shows that the TV-track point was significantly east of the radar-track point. This was caused by the TV-net choosing to track a portion of the ion cloud close to the head of the cloud (also called the hard edge or trailing edge); the radar, however,

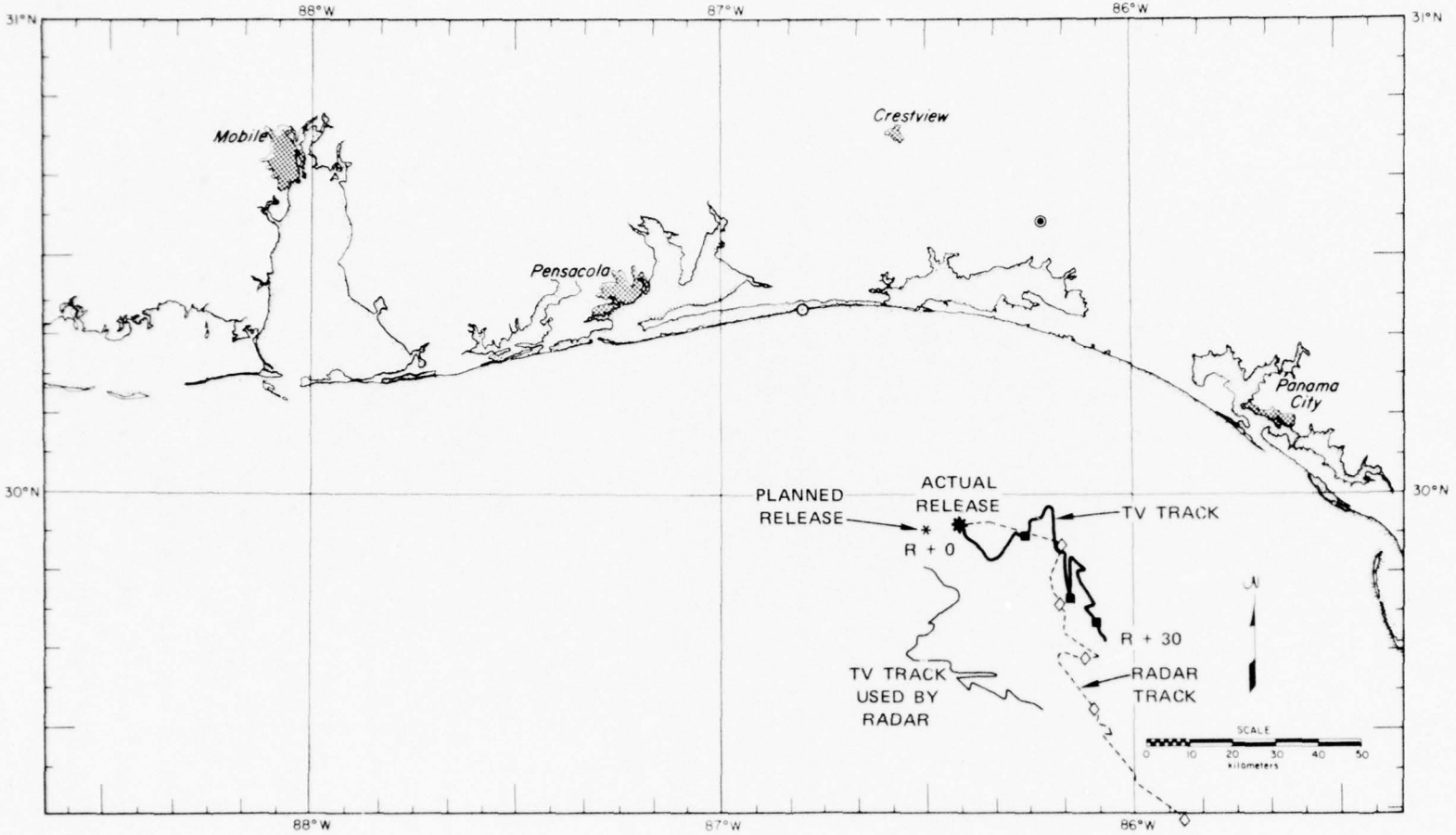

FIGURE 7 TV AND RADAR TRACKS OF ION CLOUD — EVENT ANNE

automatically gravitated toward the most dense part of the cloud (integrated over the radar-beam volume). This discrepancy was accepted as a genuine difference between the two methods of tracking and no attempt was made to force a common track point for the two systems for the later events.

Also shown in Figure 7 is the erroneous TV-track location used by the FPS-85 computer in its computation of an optically-determined ground shadow. This erroneous track was generated when the computer software interchanged the east-west and north-south displacements of the TV cloud track point from the anticipated cloud-release-point.

The track of event BETTY, shown in Figure 8, is much smoother than the ANNE track; it shows the track-smoothing effect of the empirical-height solution (for BETTY the empirical height solution placed the cloud at a constant altitude of 185 km). The radar lost the cloud just after release and did not reacquire it until R + 40 minutes, a time period indicated by the light dashed line in Figure 7. Since the dashed line is only an extrapolation between two known radar locations, the disagreement between it and the TV track is not judged to be significant. The nonuniform cloud velocity indicated by the differing distance between 10-minute marks on the TV track was caused by changing the portion of the ion cloud tracked by the TV net. As mentioned above, the TV-track cloud location data used by the FPS-85 was again in error, in this case because of an interchange of cables connecting the TV-interface unit to the FPS-85 computer.

The TV-track for event CAROLYN, shown in Figure 9, agrees quite well with the radar track. Since the radar track point automatically gravitated to the highest-average-electron-density portion of the ion cloud, this agreement shows that during the optical lifetime of this well-behaved event, the striated head of the cloud must have retained a high average electron density.

Event DIANNE, shown in Figure 10, presents a different behavior. At R + 38 minutes, when the radar came back on line (following a computer failure), it was reset to the optical track point. The radar track then moved west, not because the cloud was moving west, but because the radar

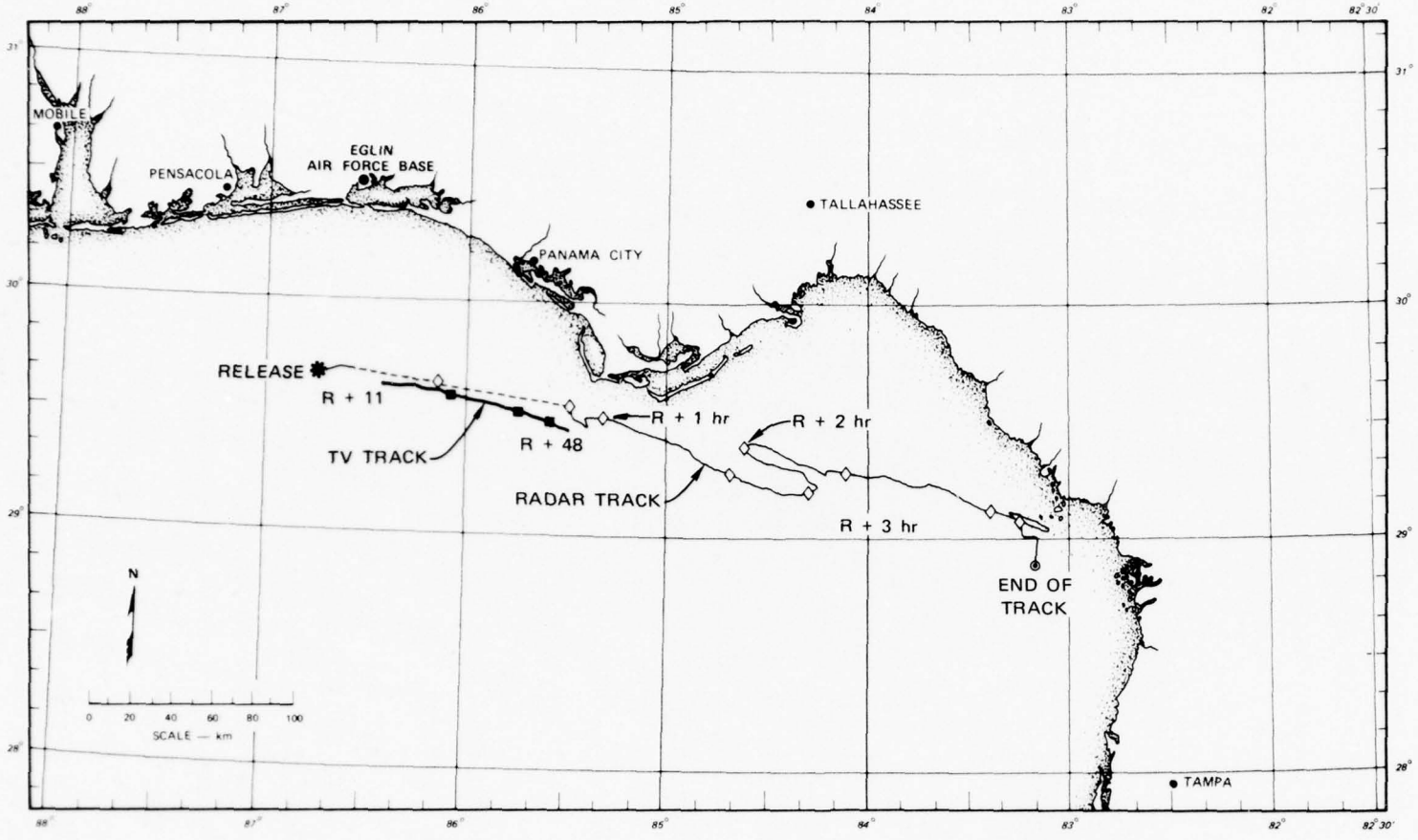

FIGURE 8 TV AND RADAR TRACKS OF ION CLOUD — EVENT BETTY

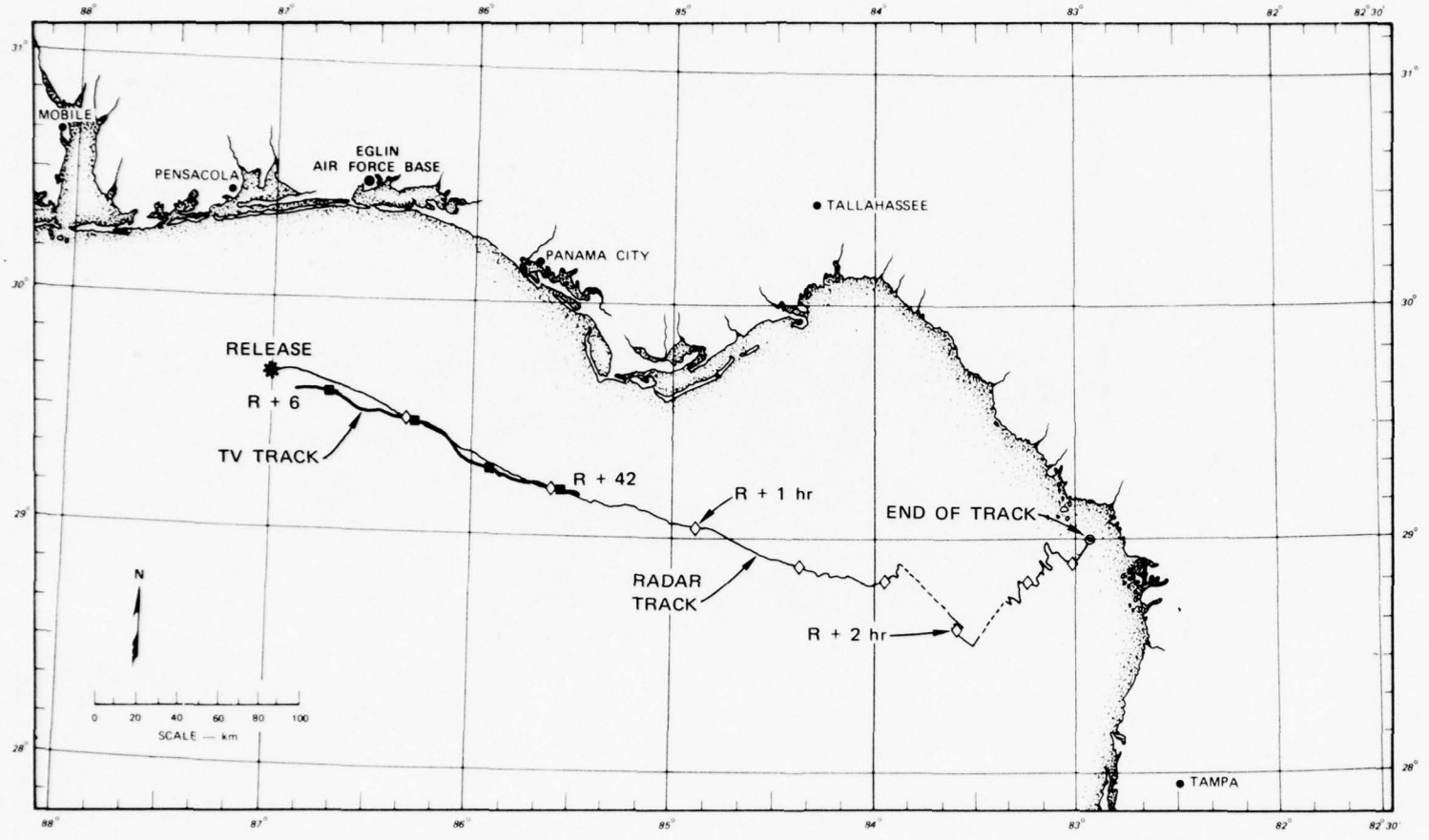

FIGURE 9 TV AND RADAR TRACKS OF ION CLOUD — EVENT CAROLYN

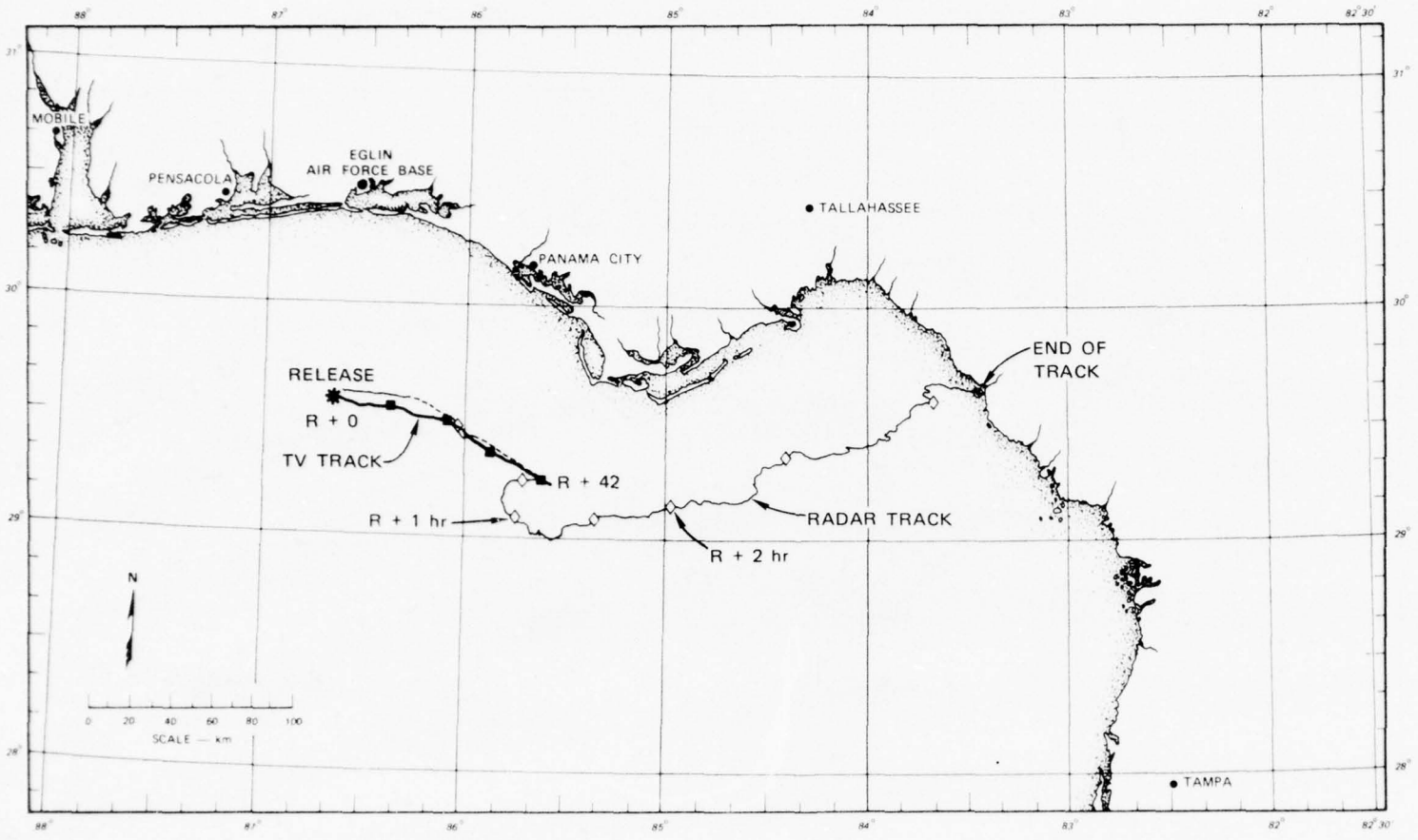

FIGURE 10 TV AND RADAR TRACKS OF ION CLOUD — EVENT DIANNE

was automatically seeking the region of highest average electron density. The radar settled down and began a reasonably smooth eastward motion at a point considerably to the west of the extrapolated optical track. This shows that the center of the striated region tracked optically was not the region with the highest average density for DIANNE.

The track of event ESTHER, shown in Figure 11, portrays the later stages of another well-behaved ion cloud with the radar track being quite smooth during the optical-cloud lifetime. The initial eastward bias of the optical track is caused by the eastern end of the cloud having the greatest contrast in the early twilight, and thus appearing as the best target to an optical system. The optical-track moves closer to that of the radar as the overall structure of the cloud becomes more apparent in the darkening sky. In the case of ESTHER, where LES-8 was the transmitting satellite (as opposed to LES-9 for releases ANNE through DIANNE), it was convenient to give the optically-derived cloud-shadow track on the same plot, as indicated by the line marked "shadow."

The optical track of event FERN, shown in Figure 12, is east of the radar track, apparently (as discussed earlier) because the TV-net was tracking the ion bridge. The erratic nature of the radar track resulted from intermittent attempts to manually reset the radar to overcome severe RFI interference problems.[3]

C. Comparison of Optical and Radio Data

To aid in the interpretation of optical and radio data, overlays of azimuth and elevation were generated for selected barium cloud photographs.* These overlays were generated by a computer program that used the right ascension and declination of the stars, the location of the viewing station, the time and date of the photographs, and the location of three reference stars in some convenient cartesian-coordinate system appropriate to the pictures. With these inputs, a full-size computer plot was

---

*The photographs used in this section were graciously provided by Technology International Corp.

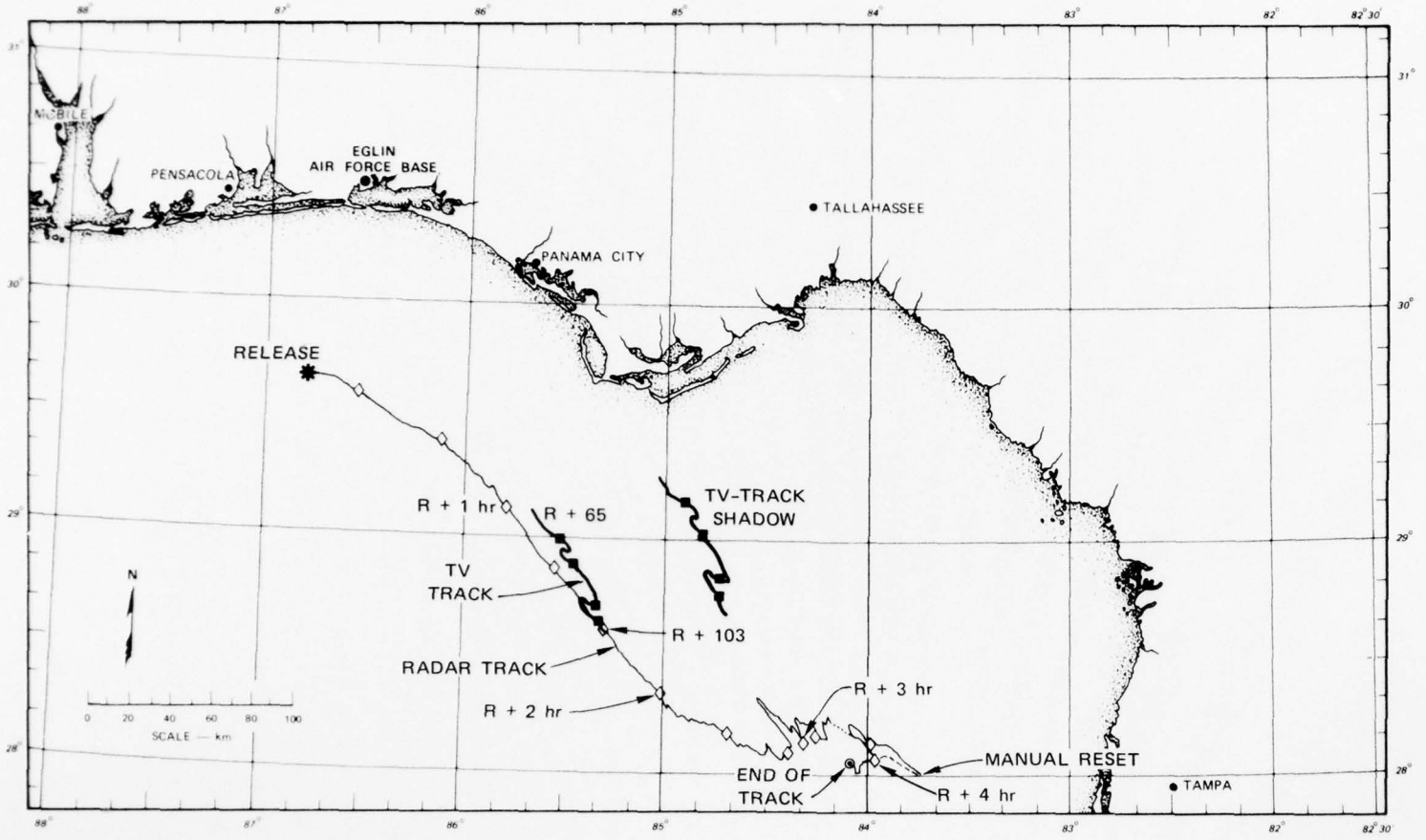

FIGURE 11 TV AND RADAR TRACK OF ION CLOUD — EVENT ESTHER

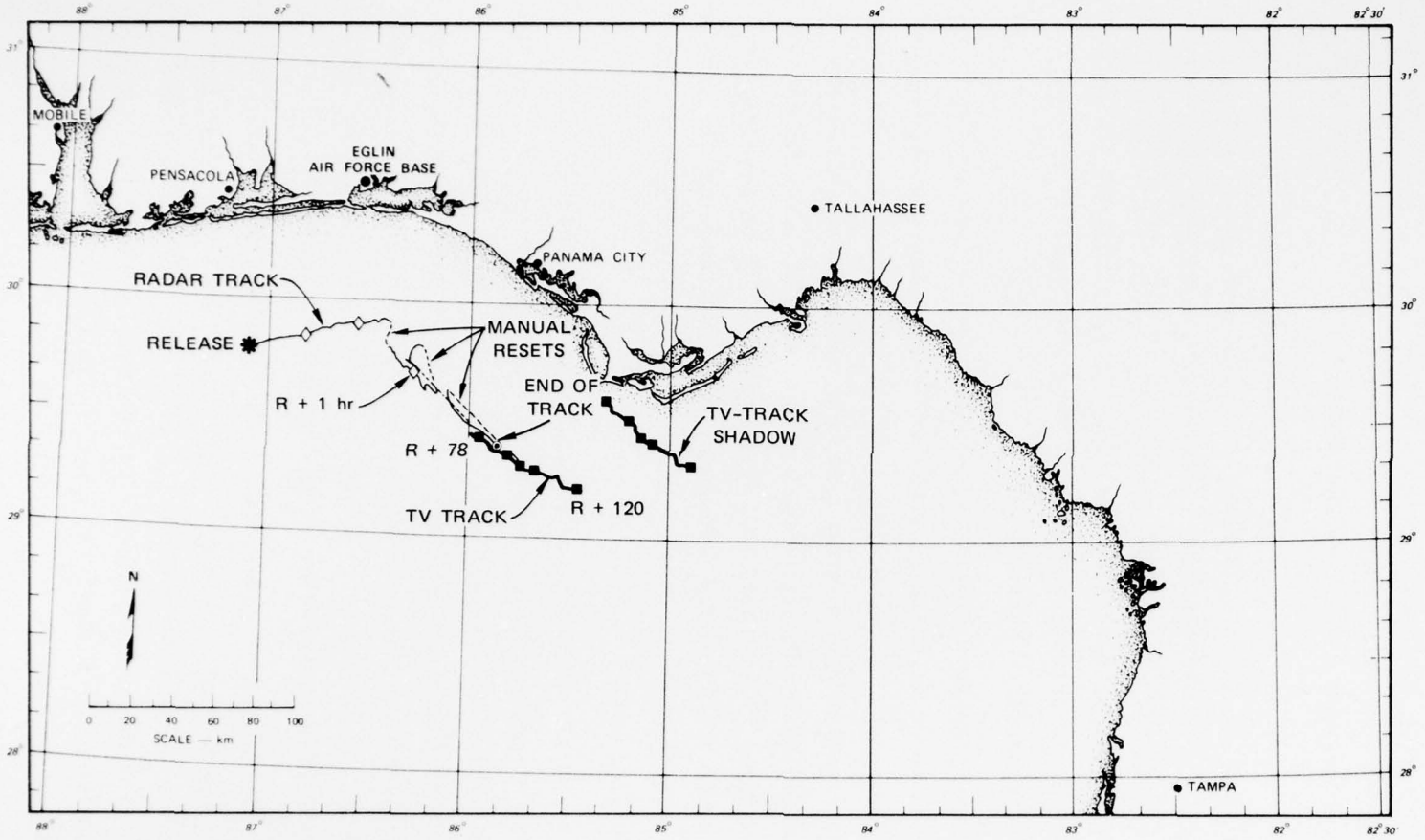

FIGURE 12 TV AND RADAR TRACKS OF ION CLOUD — EVENT FERN

generated for each photograph showing the positions of the stars in the field of view along with lines of constant azimuth and curves of constant elevation referenced to the viewing station.

The accuracy of the overlays was judged by comparing the computer-generated star locations with those in the photographs. In all cases considered in this section, the computer-generated star positions agreed with the actual ones in the photographs to within 0.1% in angular position. This accuracy was sufficient for our purposes and since photographic paper stretch can introduce errors of this magnitude no attempt was made to further refine the overlays.

The photographic overlays and the parameters used in generating them provided the means of plotting radar or TV pointing directions (azimuth and elevation) on selected pictures of the barium cloud. The trajectory of the probe rocket viewed from different photographic sites was expressed in terms of azimuth and elevation from the site of interest and plotted on the overlays. With these variables plotted, it is possible to better appreciate the relationship between measurements made by the various radio sensors and our physical view of the barium ion cloud gained largely through optical data.

Two types of radar-derived density data are presented in this section. One type is a plot of electron density (analogous to barium ion density because of charge neutrality) as a function of range for a particular radar pointing direction and time. These plots typically represent at least a 1-second average over 40 pulses. The background ionosphere has been removed, so that what is shown is the excess ionization above the normal ionosphere contributed by the barium ion cloud.

The second type of radar data shows fluctuations in electron density as a function of range for a particular radar look angle and time. These curves were generated by subtracting a "smooth" profile from the unfiltered cloud profiles mentioned above. The residue, shown as the "fluctuations" curves, is believed related to structure (striations) within the ion cloud. Because the procedure used in calculating the fluctuations involves a difference between large quantities, it was particularly error sensitive

and random noise-like peaks can appear. To minimize this type of noise, fluctuations for ESTHER were averaged over four records. FERN, however, was plagued with propagated noise that could not be removed by averaging. Thus, fluctuations for FERN are unaveraged. In either case, the peaks were considered significant only if they persisted over a number of records and if they changed in range with antenna motion.

The "point" tracked by the TV-track operator is also shown in each picture. Comparison of the TV-track point and radar measurements shows how successful the TV-track system was in locating and tracking the region of maximum electron density within the ion cloud. In addition, the juxtaposition of radar measurements with the ion cloud gives a guide in the interpretation of the radar data in terms of our physical picture of the cloud.

1. Event DIANNE

Six probe rockets were launched during STRESS to provide in situ electron density measurements of the ion cloud. Although all six probes launches during DIANNE, ESTHER, and FERN (two probes for each barium release) apparently penetrated the general volume of the ion cloud, the penetration generally occurred at times of poor or no optical coverage. The one exception was the second probe launched during DIANNE, probe flight 51-2. This probe entered the cloud around 0034:30 and measured a peak density of 1.4×10^{12} el/m^3 at a height of 182.71 km. Although the FPS-85 was inoperative at this time because of a power failure, we estimate from measurements before and after the power failure that the peak density within the ion cloud was at least 4×10^{12} el/m^3.

To determine the region probed by the rocket, consider its flight as viewed from C-6, Grayton Beach, and Tyndall. Six points on the rocket trajectory are shown in each frame of Figure 13. The point identified with a "square" is the position of the probe when it first encountered an increase in ionization above the normal background ionosphere. The other points starting from this origin locate other significant features along the rocket path as summarized in Table 2.

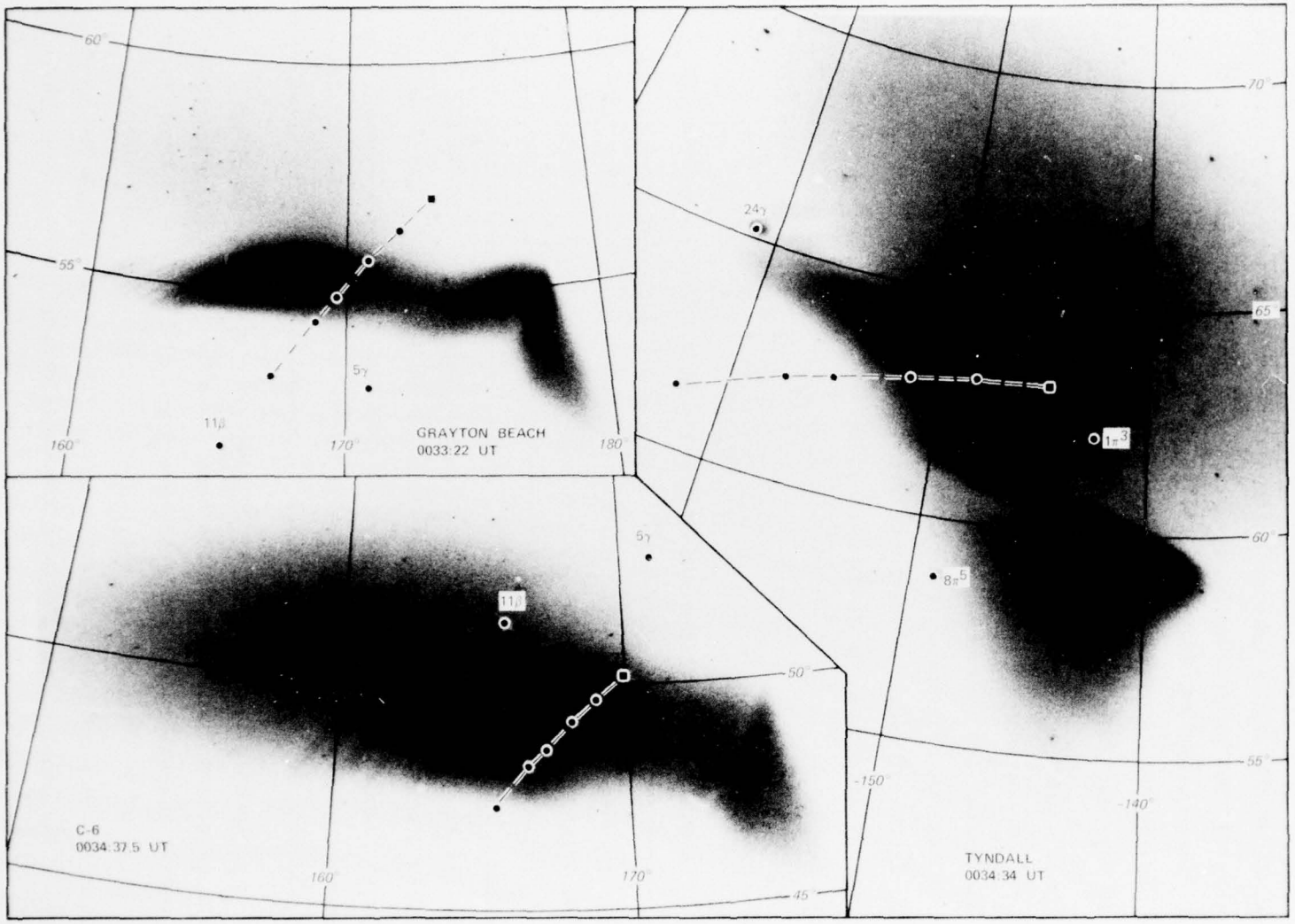

FIGURE 13 EVENT DIANNE: MONTAGE OF PHOTOGRAPHS SHOWING TRAJECTORY OF ROCKET PROBE 51-2

Table 2

SUMMARY OF SIGNIFICANT POINTS
ALONG TRAJECTORY OF PROBE 51-2

Point	Time (UT)	Height (km)	Remarks
1	0034:30.6	171.41	Cloud entry
2	0034:35.6	175.07	
3	0034:40.6	178.51	Sheet entry
4	0034:46.6	182.33	Peak density
5	0034:50.6	184.71	Sheet exit
6	0034:59.6	189.52	Cloud exit

A necessary condition for the points shown in Figure 13 to lie within the volume of the ion cloud defined by the photograph is that all corresponding points lie on the ion cloud. We emphasize, however, that the actual extent of the ion cloud cannot be sharply delineated and that the photographic extent of the cloud is a function of exposure time and geometry. That is, the pictures may show regions of high illumination and not necessarily regions of high electron densities. Nevertheless, it is useful to interpret the rocket probe data in terms of its position with respect to the photographs.

With the above criterion, the Tyndall view shows immediately that points 4, 5, and 6 lie outside of the visible cloud. A similar conclusion can be drawn for points 1 and 2 from the Grayton Beach photograph. Although we can conclude that point 3 probably lies in the cloud, this conclusion is weakened by the proximity of the point to the top edge of the cloud in the Grayton Beach photograph. In fact, since maximum density is measured at point 4, which clearly lies outside of the cloud, we conclude that probe 51-2 did not penetrate the volume of the ion cloud as defined in Figure 13. Thus, there is no inconsistency in the lower electron density measurement made by the probe in comparison with the FPS-85 measurements.

2. Event ESTHER

ESTHER was an important event because of the transmission effects that it produced. Both rocket probes recorded highly structured data, but unfortunately no optical data are available during the time of the probes. Figure 14 shows ESTHER at a time (0035 UT) when photographic and radar data were particularly good. In addition this time is of interest because strong fading was encountered by the aircraft.

The region probed by the FPS-85 was generally limited to the lower portion of the cloud around point "A." A typical radar-derived electron density profile along the radar line-of-sight "A" and the corresponding fluctuation curve, which reveals five well defined "striations," are shown above the photographs. Projection of the radar line of sight through point "A" onto the Tyndall view shows that the peaks in the fluctuations do bear a close relationship to striations in the ion cloud.

We have also picked a point "B" in the upper portion of the ion cloud not probed by radar which appears to pierce a rather distinct striation-like feature. Projection of this line of sight on the Tyndall photograph, however, does not single out any particular striation. (Points B_1 through B_4 were chosen to be at ranges of 240, 260, 280, and 300 km, respectively, from C-6.) In contrast to points A_1 through A_5, which we know because of the radar-derived range information lie in the barium cloud, we do not know the status of any of the four B points. Thus, while it is probably correct to associate A_5 with that distinct feature which also appears to lie behind α, we cannot draw similar conclusions for any of the B points. This points out the difficulty of locating an object in space without range information.

3. Event FERN

Event FERN was the most interesting of the six releases from a phenomenology point of view. The first rocket probe first encountered the cloud at an altitude of about 130 km and apparently remained in an enhanced region until an altitude of 210 km. FERN also produced strong E- and F-region returns on the vertichirp radar. These returns persisted for many tens of minutes and had a frequency extent up to 18 MHz.

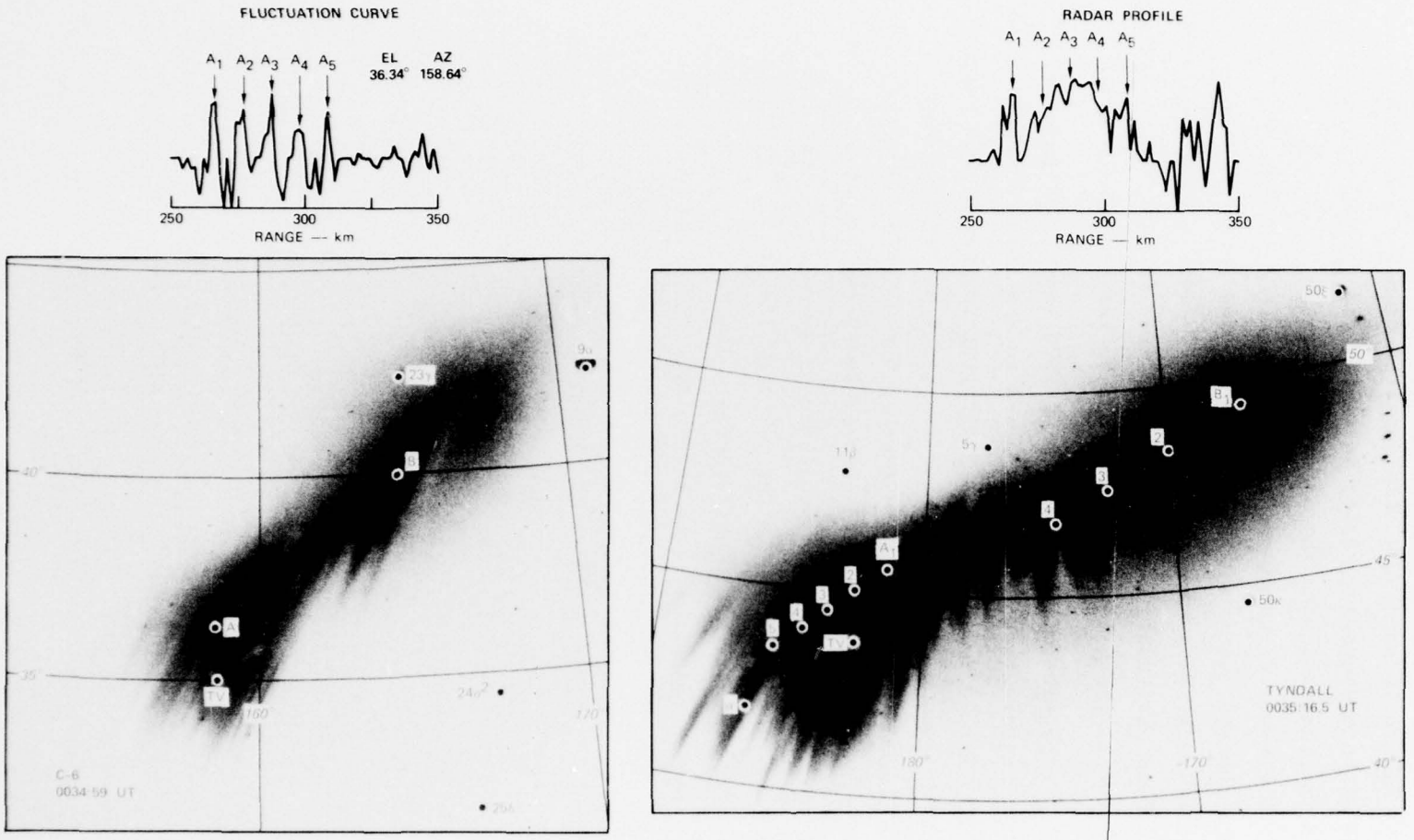

FIGURE 14 THE ESTHER CLOUD AROUND 0035 UT AND THE RADAR SIGNATURES THAT IT PRODUCED

Figure 15 shows how FERN appeared from C-6 and Tyndall. The radar data, both electron density profiles, and fluctuation curves are shown in the inserts. The sharp peak at a range of 187 km is not understood, but because it remained stationary in range as the radar pointing angle was changed, it is believed to be a noise peak and not cloud related. The radar data also show significant peaks around the 150-km range (106-km altitude). Some of the features in this region are probably related to the E-layer returns seen by the Vertichirp radar.

Inspection of the C-6 view of FERN shown in Figure 15 reveals a distinct feature that extends down and to the left and which we have identified with an "A" and a "B." In trying to locate this feature on the Tyndall view, we have projected the lines of sight through A and B onto the Tyndall picture. The extreme point on each projection delineates the extent of the cloud as determined by the measured electron density profiles. From these projections, we conclude that the bulk of the ion cloud above point B in the C-6 view lies to the right and outside the field of view of the Tyndall camera. The feature of interest in the C-6 view thus appears to be such a big object that it occupies almost the entire field of view in the Tyndall photograph.

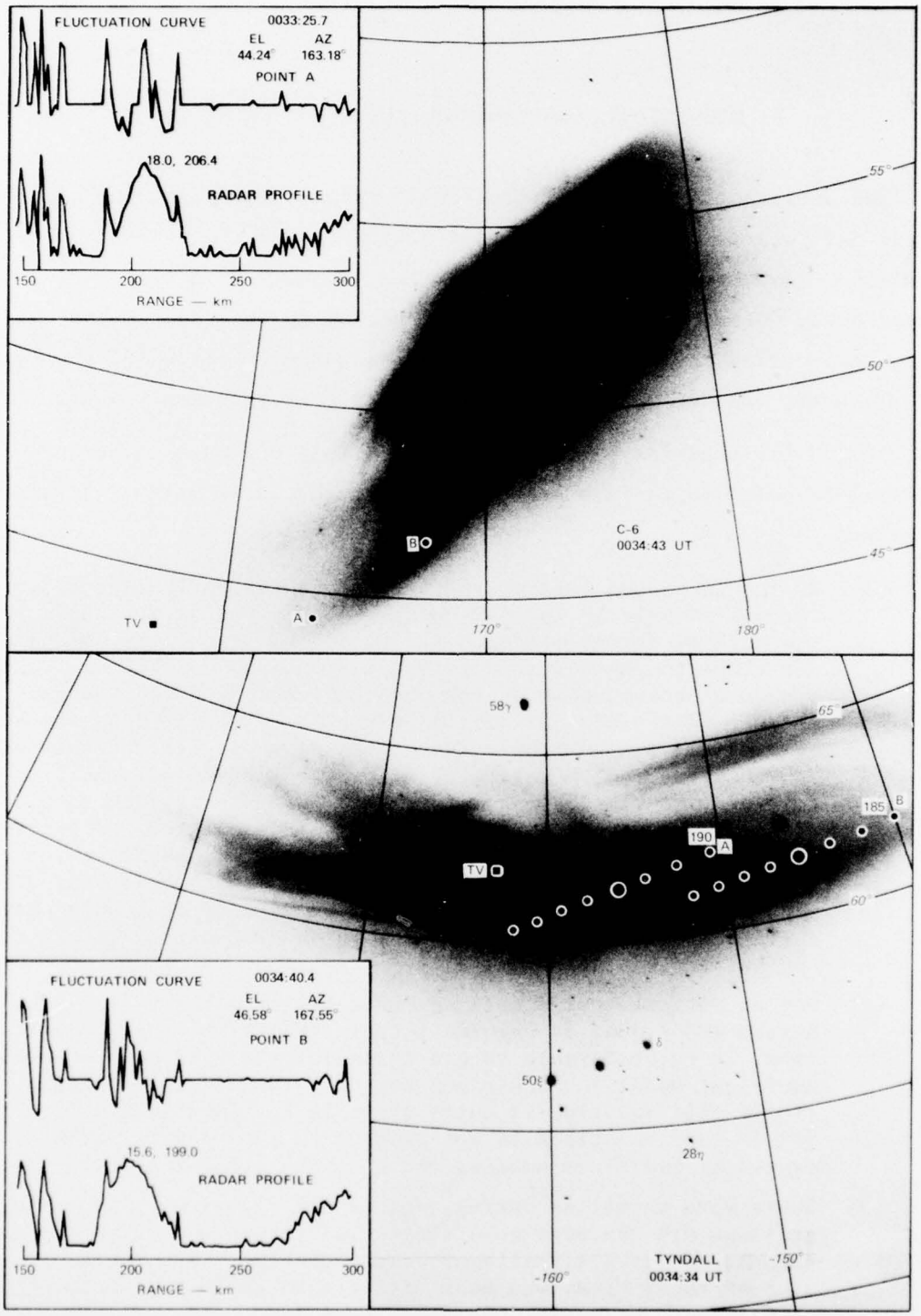

FIGURE 15 FERN AROUND 0035 UT AND ASSOCIATED RADAR SIGNATURES

V DISCUSSION, CONCLUSIONS, AND RECOMMENDATIONS

The outstanding success of the FPS-85 radar in tracking the STRESS clouds has largely relegated optical-tracking systems to a backup role if similar test series are performed in the future. An optical-track system does, however, provide acceptable backup to the radar. Furthermore, it provides a means for the radar to acquire or reacquire the cloud if, as in the case of event DIANNE, the radar gets hopelessly lost.

The TV-track system performance in the field and post-event data analysis have led to certain conclusions that should be noted for future reference.

(1) As the ion cloud evolves in time, or as its entire structure becomes visible in the darkening sky, any optical tracking system will be forced occasionally to switch track from one part of the cloud to another in a rather discontinuous fashion. This is a natural consequence of the physical processes operating on the cloud, and the discontinuities cannot be eliminated by any sort of predictive algorithm. The effect of these discontinuities can be mitigated, however, by a more sophisticated algorithm for relaying cloud-track information to a user. Such an algorithm should probably be structured to account for the finite extent of the cloud in the horizontal direction, and the general location of the chosen track point within that horizontal dimension. A detailed study of the wide variety of clouds observed during STRESS will be very useful in developing any future optical-track systems.

(2) For an optical system used to track the striated region of a barium ion cloud, as opposed to point-tracking a single striation, it is preferable to use a single-site system with an empirical model for the cloud height. The accuracy of such a single-site solution is quite adequate for experiments like STRESS, and the track is not subject to the random fluctuations caused by two sites hunting for a common aim point in the cloud.

(3) There were occasions during some of the events when two or more stations did converge on a single identifiable feature and maintain track for a significant period of time. The track precision at these times was much higher than could have been obtained from the radar. On other occasions (e.g., DIANNE), the optical system was tracking trailing-edge striations that were

not seen by the radar because the average electron density in the radar beam was too low. Although the precision track and the low-density-region track capabilities of the optical system were not important in STRESS, they may be in some future experiments. For a reliable and consistent precision track, however, it is absolutely essential that the central-site operator be supplied with the video from the other participating sites. Only by looking at all views of the cloud can he hope to develop a mental picture of the three-dimensional shape of the cloud, and intelligently direct aimpoint changes in the various sites. A larger field of view than used for STRESS would also be needed for accommodating late-time barium releases.

REFERENCES

1. S. P. Geller and T. N. Davis, "Tracking Barium Releases Using the TV-Track System," Technical Report No. 2, Contract F-30602-70-C-0179, University of Alaska, College, AK (May 1971).

2. D. R. McDaniel, "STRESS Preliminary Field Test Plan," SRI International Memorandum prepared for Director of the Defense Nuclear Agency, Washington, D.C., SRI Project 4769, SRI International, Menlo Park, CA (May 1976).

3. V. Gonzalez, "Project STRESS--Radar Tracking of Ion Clouds," Interim Technical Report 1, Contract DNA001-76-C-0341, SRI Project 5575, SRI International, Menlo Park, CA (July 1977).

DISTRIBUTION LIST

DEPARTMENT OF DEFENSE

Director
Command Control Technical Center
ATTN: C-650

Director
Defense Advanced Rsch. Proj. Agency
ATTN: Nuclear Monitoring Research
ATTN: Strategic Tech. Office

Defense Communication Engineer Center
ATTN: Code R410, James W. McLean

Director
Defense Communications Agency
ATTN: Code 480
ATTN: Code 810, R. W. Rostron
ATTN: Code 101B, Major Rood

Defense Communications Agency
WWMCCS System Engineering Org.
ATTN: R. L. Crawford

Defense Documentation Center
Cameron Station
12 cy ATTN: TC

Director
Defense Nuclear Agency
ATTN: TISI, Archives
ATTN: DDST
ATTN: STVL
3 cy ATTN: TITL, Tech. Library
3 cy ATTN: RAAE

Commander
Field Command, Defense Nuclear Agency
ATTN: FCPR

Director
Joint Strat Tgt. Planning Staff
ATTN: JLTW-2

Chief
Livermore Division, Fld. Command, DNA
ATTN: FCPRL

Director
National Security Agency
ATTN: John Skillman, R52
ATTN: W14, Pat Clark

Commandant
NATO School (SHAPE)
ATTN: U.S. Documents Officer

Under Sec'y of Def. for Rsch. & Engrg.
ATTN: S&SS (OS)
ATTN: AE

DEPARTMENT OF THE ARMY

Director
BMD Advanced Tech. Ctr., Huntsville Office
ATTN: ATC-T, Melvin T. Capps

DEPARTMENT OF THE ARMY (Continued)

Commander
Harry Diamond Laboratories
ATTN: Mildred H. Weiner, DELHD-TI
ATTN: Francis N. Wimenitz, DELHD-NP
2 cy ATTN: DELHD-NP

Commander
US Army Nuclear & Chemical Agency
ATTN: Library

Commander
US Army SATCOM Agency
ATTN: Doc. Control

DEPARTMENT OF THE NAVY

Chief of Naval Research
ATTN: Code 461

Commanding Officer
Naval Intelligence Support Ctr.
ATTN: Mr. Dubbin, STIC 12

Commander
Naval Ocean Systems Center
ATTN: Code 532

Director
Naval Research Laboratory
ATTN: Code 7730, Edgar A. McClean
ATTN: Code 5410, John Davis
ATTN: Code 6701, Jack D. Brown
ATTN: Code 5430, Satellite Comm.
ATTN: Code 6700, Timothy P. Coffey
ATTN: Code 5400, HG. Comm. Dir., Bruce Wald

Officer-in-Charge
Naval Surface Weapons Center
ATTN: Code WA501, Navy Nuc. Prgms. Off.

Director
Strategic Systems Project Office
ATTN: NSSP-2722, Fred Wimberly
ATTN: NSP-2141

DEPARTMENT OF THE AIR FORCE

AF Geophysics Laboratory, AFSC
ATTN: PHD, John P. Mullen
ATTN: OPR-1, James C. Ulwick
ATTN: PHD, Jurgen Buchau
ATTN: SUOL Rsch. Lib.
ATTN: PHP, Jules Aarons

AF Weapons Laboratory, AFSC
ATTN: SUL
ATTN: DYT, Capt L. Wittwer
ATTN: DYC, John M. Kamm

AFTAC
ATTN: TN

Air Force Avionics Laboratory, AFSC
ATTN: AAD, Allen Johnson

DEPARTMENT OF THE AIR FORCE (Continued)

Headquarters
Electronic Systems Division, (AFSC)
ATTN: Jim Deas

Commander
Foreign Technology Division, AFSC
ATTN: NICD Library

Commander
Rome Air Development Center, AFSC
ATTN: FMTLD, Doc. Library

SAMSO/MN
ATTN: MNNL, Lt Col Kennedy

SAMSO/SK
ATTN: SKA, Lt Maria A. Clavin

SAMSO/YA
ATTN: YAT, Capt L. Blackwelder

Commander in Chief
Strategic Air Command
ATTN: XPFS, Maj Brian G. Stephan
ATTN: ADWATE, Capt Bruce Bauer
ATTN: NRT

DEPARTMENT OF ENERGY

University of California
Lawrence Livermore Laboratory
ATTN: Tech. Info. Dept., L-3

Los Alamos Scientific Laboratory
ATTN: Doc. Con. for Robert Jefferies
ATTN: Doc. Con. for John Wolcott
ATTN: Doc. Con. for John Zinn

Sandia Laboratories
ATTN: Doc. Con. for T. Wright
ATTN: Doc. Con. for D. A. Dahlgren, Org. 1722
ATTN: Doc. Con. for J. P. Martin, Org. 1732

OTHER GOVERNMENT AGENCIES

Department of Commerce
Office of Telecommunications
ATTN: William F. Utlaut

National Oceanic & Atmospheric Admin.
Environmental Research Laboratories
ATTN: C. L. Ruffnach

DEPARTMENT OF DEFENSE CONTRACTORS

Aerospace Corporation
ATTN: T. M. Salmi
ATTN: SMFA for PWW
ATTN: Irving M. Garfunkel
ATTN: Norman D. Stockwell
ATTN: J. E. Carter, 120, Rm. 2209

University of California at San Diego
ATTN: Henry G. Booker

COMSAT Laboratories
ATTN: R. R. Taur

DEPARTMENT OF DEFENSE CONTRACTORS (Continued)

Cornell University
Department of Electrical Engineering
ATTN: D. T. Farley, Jr.

ESL, Inc.
ATTN: James Marshall
ATTN: C. W. Prettie

General Electric Company
TEMPO-Center for Advanced Studies
ATTN: DASIAC
ATTN: Warren S. Knapp

General Electric Company
ATTN: F. A. Reibert

General Research Corporation
ATTN: Joel Garbarino
ATTN: John Ise, Jr.

Geophysical Institute
University of Alaska
ATTN: Tech. Library

University of Illinois
Department of Electrical Engineering
ATTN: K. C. Yeh

Institute for Defense Analyses
ATTN: Ernest Bauer

Intl. Tel. & Telegraph Corporation
ATTN: Tech. Library

JAYCOR
ATTN: S. R. Goldman

Johns Hopkins University
Applied Physics Laboratory
ATTN: Thomas Potemra
ATTN: Doc. Librarian
ATTN: John Dassoulas

M.I.T. Lincoln Laboratory
ATTN: LIB A-082 for David M. Towle

McDonnell Douglas Corporation
ATTN: Tech. Library Services

Mission Research Corporation
ATTN: F. Fajen
ATTN: D. Sappenfield
ATTN: R. Bogusch
ATTN: Ralph Kilb
ATTN: Dave Sowle
ATTN: R. Hendrick

The Mitre Corporation
ATTN: Chief Scientist, W. Sen

Physical Dynamics
ATTN: E. J. Fremouw

Physical Dynamics, Inc.
ATTN: Joseph B. Workman

DEPARTMENT OF DEFENSE CONTRACTORS (Continued)

R & D Associates
ATTN: William J. Karzas
ATTN: Bryan Gabbard
ATTN: Robert E. Lelevier

The Rand Corporation
ATTN: Ed Bedrozian
ATTN: Cullen Crain

Raytheon Company
ATTN: Barbara Adams

Science Applications, Inc.
ATTN: Lewis M. Linson
ATTN: Daniel A. Hamlin
ATTN: D. Sachs

DEPARTMENT OF DEFENSE CONTRACTORS (Continued)

SRI International
ATTN: Ray L. Leadabrand
ATTN: Charles L. Rino
ATTN: Walter G. Chesnut
ATTN: Dan McDaniel
ATTN: Victor Gonzales
ATTN: Norman J. F. Chang
ATTN: Richard D. Hake, Jr.

Technology International Corporation
ATTN: W. P. Boquist